MAST4 regulates spermatogonial stem cell self-renewal controlling cell cycle via the FGF2/ERM pathway

Seung-Jun Lee

The Graduate School
Yonsei University
Department of Applied Life Science

MAST4 regulates spermatogonial stem cell self-renewal controlling cell cycle via the FGF2/ERM pathway

Directed by Professor Han-Sung Jung

A Dissertation Thesis
Submitted to the Department of Applied Life Science
and the Graduate School of Yonsei University
in partial fulfilment of the requirements
for the degree of Doctoral Philosophy

Seung-Jun Lee

December 2023

This certifies that the Doctoral Dissertation of Seung-Jun Lee is approved.

_____

Han-Sung Jung

_____

Na-Young Song

_____

Jong-Min Lee

_____

Kye-Seong Kim

_____

Jonghoon Choi

The Graduate School

Yonsei University

December 2023

Acknowledgement

본 학위논문이 나오기까지 많은 분들의 조언과 도움이 있었습니다. 학위 기간 동안 저의 부족한 점들을 정성껏 지도해주시고 진정한 학자로 거듭날 수 있게 해 주신 정한성 교수님께 깊은 존경의 마음과 감사를 드립니다. 저의 대학원 생활을 잘 이끌어 주시고 논문 작성에도 많은 도움을 주신 이종민 박사님 감사드립니다. 바쁘신 와중에도 논문의 미비한 점을 지도해주신 송나영 교수님, 김계성 교수님, 최종훈 교수님께도 감사를 드립니다. 또한 대학원 생활을 버텨내고 앞으로 나아갈 수 있도록 큰 힘이 되어준 김은정 박사님께 감사를 드립니다. 대학원 생활 내내 동고동락하며 지지와 격려를 아끼지 않고 잘 버틸 수 있게 도와준 Adpaikar Anish Ashok 박사님, Li Shujin 선생님 감사를 드립니다. 밝은 웃음과 친절함으로 교실 생활의 어려움을 잊게 해 주신 김민정 선생님, Cui Yan 선생님, Baskaran Senthil Kumar, 김지선 선생님께도 감사의 말을 전합니다. 끝으로 대학원 생활 동안 끝까지 힘이 되어 준 모든 친구들과 짧지 않은 시간임에도 묵묵히 응원과 격려를 아끼지 않으신 부모님을 비롯 가족 모두에게 감사의 인사를 전합니다.

2023년 12월

저자 씀

TABLE OF CONTENTS

LIST OF FIGURES iv
LIST OF TABLES ..... **vi**
LIST OF ABBREVIATIONS ..... **vii**
ABSTRACT ..... **ix**
I. INTRODUCTION **1**
1. Stem cell 1
1.1 Origin of stem cells 1
1.2 Stem cell characterization 2
1.3 Self-renewal and differentiation 3
1.4 Tissue-specific stem cell maintenance 5
1.5 Stem cell niche 6
2. Cell cycle 9
2.1 Cell cycle progression and cyclin-CDK complexes 9
2.2 Cell cycle controlling stem cell self-renewal 12
3. Spermatogenesis 14
3.1 Testis development 16
3.2 Meiosis 17
4. SSC self-renewal 18
4.1 SSCs 18
4.2 Sertoli cells 19
4.3 Sertoli cell-only (SCO) syndrome 21
5. Microtubule-associated serine/threonine kinase family member 4 (MAST4) 22
6. Aim of this study 23
II. MATERIALS AND METHODS **24**
1. Animals 24
2. Histology 28
2.1 Wax section 28
2.2 Hematoxylin and Eosin (HE) 28

3. Immunohistochemistry (IHC) 29
4. Section *in situ* hybridization 31
5. 5'-iodo-2'-deoxyuridine (IdU)/5'-bromo-2'-deoxyuridine (BrdU) injection and cell cycle time (T_c) calculation 31
6. Testis tissue culture 35
7. Cell culture and lentivirus transduction 37
8. Protein extraction, nuclear/cytoplasmic fractionation and western blot 38
9. Immunoprecipitation (IP) 40
10. RNA preparation, reverse transcription-polymerase chain reaction (RT-PCR) and real time-quantitative polymerase chain reaction (RT-qPCR) analysis 42
10.1 RNA preparation 42
10.2 Reverse Transcription 43
10.3 RT-PCR 43
10.4 RT-qPCR 43
11. RNA sequencing (RNA-seq) analysis 46
12. Luciferase assay 47
13. Terminal deoxynucleotidyl transferase dUTP nick end labeling (TUNEL) staining 48
14. Sperm count 48
15. Statistical analysis 49
III. Section I: MAST4 activates ERM in Sertoli cells for SSC self-renewal 50
1. Introduction 50
2. Results 52
2.1. Spermatogenic dysregulation in *Mast4* KO testes 52
2.2. MAST4 expression pattern during spermatogenesis 54
2.3. Irregular seminiferous tubule structures in *Mast4* KO testes 58
2.4. Sertoli cell-only tubule phenotype in *Mast4* KO testes 60
2.5. Differences in cell proliferation and apoptosis in *Mast4* KO testes 63
2.6. Effects of MAST4 on ERM transcription factor 65
2.7. Regulation of genes related to SCC self-renewal via the MAST4–ERM interaction 68

2.8. MAST4-mediated phosphorylation of ERM at serine 367 72
3. Discussion 76
IV. Section II : MAST4 controls cell cycle in SSCs 78
1. Introduction 78
2. Results 80
2.1. MAST4-induced regulation of SSC self-renewal 80
2.2. Cell cycle alteration of SSCs in *Mast4* KO testes 82
2.3. Effects of MAST4 on the mechanism involved in the cell cycle of SSCs ... 84
2.4. Increased interaction of PLZF and CDK2 by CXCL12 87
2.5. FGF2/MAST4/CXCL12 pathway on the seminiferous tubular structure 89
2.6. FGF2/MAST4/CXCL12 pathway on the cell cycle of SSCs 92
3. Discussion 94
V. GENERAL DISCUSSION 96
VI. CONCLUSION 98
ABSTRACT (In Korean) 109
PUBLICATION LIST 111

LIST OF FIGURES

Figure 1. Niche cells controlling the self-renewal of stem cells..... 8
Figure 2. Cell cycle progression and cyclin–CDK complexes..... 11
Figure 3. Structure of seminiferous tubules and spermatogenesis..... 15
Figure 4. Sertoli cell–Spermatogonial stem cell interaction on self-renewal and differentiation 20
Figure 5. *Mast4* genomic structure and the generation of *Mast4* KO mice 27
Figure 6. IdU/BrdU injection for cell cycle calculation..... 34
Figure 7. *In vitro* culture of mouse testis tissue using Trowell's culture..... 36
Figure 8. Analysis of testicular size and total sperm number between WT and *Mast4* KO mice..... 53
Figure 9. MAST4 expression pattern during testis development 56
Figure 10. *In situ* hybridization of *Mast4* expression during testis development 57
Figure 11. Sertoli cell-only tubular structure in *Mast4* KO and aged mouse testes..... 59
Figure 12. Comparison of testis marker expression between WT and *Mast4* KO testes..... 61
Figure 13. RNA-seq analysis in PN 6W WT and *Mast4* KO testes 62
Figure 14. Proliferative and apoptotic marker expression between WT and *Mast4* KO testes..... 64
Figure 15. Effects of FGF2 on the expression of *Mast4* and *Erm*..... 66
Figure 16. ERM expression in WT and *Mast4* KO 67
Figure 17. Interaction of MAST4 and ERM 69
Figure 18. Transcriptional activities of ERM according to FGF2 and MAST470

Figure 19. mRNA expression of *Erm* and ERM target genes according to MAST4 71
Figure 20. MAST4-mediated phosphorylation of ERM at serine 367 74
Figure 21. MAST4-mediated transcriptional activities of ERM at serine 367. 75
Figure 22. PLZF expression between WT and *Mast4* KO testes 81
Figure 23. Cell cycle analysis between WT and *Mast4* KO spermatogonial stem cells 83
Figure 24. PLZF–CDK2 interaction and MAST4-mediated CDK2 expression 85
Figure 25. Cell cycle-related gene expression between WT and *Mast4* KO testes 86
Figure 26. Effect of CXCL12 on the interaction between PLZF and CDK2 ... 88
Figure 27. Testicular structure of *Mast4* KO testes according to FGF2 and CXCL12 90
Figure 28. PLZF expression according to FGF2/MAST4/CXCL12 91
Figure 29. Cell cycle rescue of *Mast4* KO testes according to FGF2 and CXCL12 93
Figure 30. MAST4 regulates the self-renewal of spermatogonial stem cells in terms of cell cycle maintenance through the MAST4-ERM-PLZF mechanism 99

LIST OF TABLES

Table 1. Primary antibodies for Immunohistochemistry..... 30
Table 2. Primary antibodies for Western blot..... 39
Table 3. Primary antibodies for Immunoprecipitation..... 41
Table 4. Primers for RT-PCR and RT-qPCR 45

LIST OF ABBREVIATIONS

BMP	Bone Morphogenic Protein
CCL	C-C-Motif Ligand
CXCL	C-X-C-Motif Ligand
CDK	Cyclin Dependent Kinase
DPC	Days Post Coitum
DUF	Domain of Unknown Function
E	Embryonic days
ECM	Extracellular Matrix
EPSC	Epidermal Stem Cell
ERM	Ets-related Molecule
ES	Embryonic Stem
FGF2	Fibroblast Growth Factor 2
GDNF	Glial cell line-derived Neurotrophic Factor
ICM	Inner Cell Mass
iPSC	Induced Pluripotent Stem Cell
KO	Knockout
MAST4	Microtubule-associated Serine/Threonine Kinase 4
MSC	Mesenchymal Stem Cell
PAX7	Paired Box Protein 7
PDZ	Postsynaptic density protein 95 (PSD95), Discs large MAGUK scaffold protein 1 (DLG1) and Zona occludens 1 (ZO-1)

PGC	Primordial Germ Cell
PLZF	Promyelocytic Leukemia Zinc Finger
SC	Sertoli Cell
SCO	Sertoli Cell-Only
SSC	Spermatogonial Stem Cell

ABSTRACT

Spermatogenesis is an important cellular differentiation process through which the male gametes are produced, and it remains active throughout an individual's lifespan. Sertoli cell-only syndrome (SCO), including infertility, refers to the dysfunction of the male reproductive system. The self-renewal of spermatogonial stem cells (SSCs) must be accurate to prevent SCO syndrome. This study investigated the role of microtubule-associated serine/threonine kinase family member 4 (MAST4) in spermatogenesis in mice. Results revealed that MAST4 was localized in Sertoli cells before puberty, providing a somatic niche for spermatogenesis in mice. The size of *Mast4* knockout testes was reduced compared with that of wild-type testes, and germ cell depletion associated with an increase in apoptosis and subsequent loss of tubular structure were similar to the SCO phenotype. MAST4 phosphorylated the ETS-related molecule (ERM), specifically the serine 367 residue. ERM phosphorylation ultimately controlled the transcription of ERM target genes related to the self-renewal of SSCs. *Mast4* deletion led to the decreased promyelocytic leukemia zinc finger (PLZF) expression and cell cycle progression in the testes. MAST4 also induced cyclin-dependent kinase 2 to phosphorylate PLZF, and the activated PLZF suppressed the transcriptional levels of genes related to cell cycle arrest;

consequently, SSCs retained their stem cell state. Therefore, MAST4 is associated with the fibroblast growth factor 2 (FGF2)/ERM pathway, and this association helps us explore the ability of SSCs to maintain a vertebrate stem cell niche.

Key words: MAST4, Spermatogonial stem cell self-renewal, Cell cycle, ERM, PLZF

I. INTRODUCTION

1. Stem cell

1.1 Origin of stem cells

Stem cells are responsible for the organ and tissue development, growth, and maintenance from the embryonic stage up to late adult life (Bloch, 2016). Pluripotency is first acquired in the mouse embryo as the epiblast forms in the inner cell mass (ICM). These cells retain the capacity to repopulate an embryo and to contribute descendants to all adult tissues, including the germline (Bradley et al., 1984); thus, they are defined as being naïve pluripotent cells (Nichols & Smith, 2009). Embryonic stem (ES) cells have been equated to ICM cells from 3.5 days post coitum (dpc) mouse blastocysts. However, ES cells may also be derived from blastomeres isolated from mouse embryos at the eight-cell stage (Eistetter, 1989). Conclusively, Brook and Gardner demonstrated that the origin of ES cells is the early epiblast, following its overt segregation from the hypoblast (Brook & Gardner, 1997). Given that embryonic germ cells resemble ES cells, ES cells may arise from epiblast cells that are already predisposed to a primordial germ cell (PGC) fate (Zwaka & Thomson, 2005). Thus, naïve

pluripotency may likely occur from two possible origins during development: first in the early epiblast and later in the germ cell lineage.

1.2 Stem cell characterization

Stem cell markers are genes and their protein products used by scientists to isolate and identify stem cells. Although functional assays are the ideal approach to define stem cell, their molecular markers provide a systematic approach to characterize a healthy and robust stem cell population. In addition, their unique expression pattern and timing are useful tools for stem cell isolation and identification.

Two homeodomain transcription factors, namely, OCT4 (POU5F1) and NANOG, were the first proteins recognized to be essential for early embryo development and pluripotency maintenance in ES cells (Nichols et al., 1998). In addition to OCT4, SOX2, and NANOG, other factors, including SALL4, DAX1, ESSRB, TBX3, TCL1, RIF1, NAC1, and ZFP281, have been identified as necessary for pluripotency (Loh et al., 2006). These pluripotency factors regulate concomitantly to form a complicated transcriptional regulatory network in ES cells (Gifford et al., 2019, Shi et al., 2021, Zhou et al., 2007). Several cell surface markers (SSEA-1, SSEA-4, TRA-1-60, and

TRA-1-81) have been used to characterize mouse and human ES cells (BÜHRING et al., 2007).

In a major technological breakthrough in science and medicine in 2006, cells with a gene expression profile and developmental potential similar to those of ES cells can be generated from mouse somatic cells by using a cocktail of four transcription factors (Takahashi & Yamanaka, 2006). These cells were called induced pluripotent stem cells (iPSCs), and the four factors, namely, OCT4, SOX2, KLF4, and MYC, were named "Yamanaka factors." Human iPSC technology has ushered in an exciting new era for the fields of stem cell biology and regenerative medicine, as well as disease modeling and drug discovery. They have several advantages, including human origin, easy accessibility, expandability, ability to give rise to almost any cell types desired, avoidance of ethical concerns associated with human ES cells, and the potential to develop personalized medicine using patient-specific iPSCs. Therefore, the stem cell population and their characteristics should be maintained, i.e., the balance between self-renewal and differentiation.

1.3 Self-renewal and differentiation

Stem cells are defined by their ability to make more stem cells, a property known as "self-renewal," and their ability to produce cells that differentiate

(Morrison & Kimble, 2006). They can accomplish these two tasks through various strategies, such as asymmetric cell division by which each stem cell divides to generate one daughter cell with a stem cell fate (self-renewal) and another daughter cell that differentiates (Clevers, 2005). Many stem cells experience prolonged periods of quiescence throughout the life of an organism, and they can undergo self-renewal to maintain the resident stem cell population (van Velthoven & Rando, 2019).

ES cells possess a nearly unlimited self-renewal capacity and developmental potential to differentiate into virtually any cell type (Wobus & Boheler, 2005). This capacity, which is called totipotency, is retained by the early progeny of the zygote up to the eight-cell stage of the morula. Adult stem cells, which exist in postnatal organisms, are either multipotent or unipotent. The majority of known adult stem cells reside in the bone marrow. Among them are multipotent hematopoietic stem cells, which can regenerate the entire hematopoietic system (Bryder et al., 2006). Other adult stem cells that reside in the bone marrow are mesenchymal stem cells, also known as mesenchymal stromal cells (MSC), which can differentiate into the bone, chondrocytes, and adipose cells (Bianco, 2014).

1.4 Tissue-specific stem cell maintenance

Throughout the mammalian body, tissue maintenance and differentiation are ultimately regulated by coordination between the proliferation and differentiation of specific stem or progenitor cells.

Epidermal stem cells (EPSCs) are a multipotent cell type involved in the formation and differentiation of the functional epidermis (Yang et al., 2019). In the mediation of the self-renewal and differentiation of EPSCs, canonical Wnt signaling promotes the accumulation of key microtubule-binding proteins that stabilize microtubules at the wound edge in an active state to promote wound repair (Wu et al., 2011).

In human dental follicle cells, Notch1 activation may diminish the ability of stem cells to differentiate, promoting their self-renewal capacity and proliferation (Chen et al., 2013). In mouse incisors, SOX2-positive cell populations are important for self-renewal and differentiation (Sanz-Navarro et al., 2018).

In the intestine, the intestinal epithelium is characterized by its remarkable self-renewal ability, with a turnover time of 4–5 days, and LGR5-marked crypt base columnar cells represent actively proliferating stem cells that

mediate the daily renewal of the intestinal epithelium (Barker et al., 2007, Van Der Flier & Clevers, 2009). Wnt signaling is essential for the homeostatic self-renewal and proliferation of the intestinal stem cell compartment (Schuijers & Clevers, 2012). Bone morphogenetic protein (BMP) plays a pivotal role in balancing the Wnt-driven homeostatic self-renewal and proliferation of the intestinal epithelium (Clevers, 2013, Medema & Vermeulen, 2011).

1.5 Stem cell niche

The ability of stem cells to self-renew and retain their identity depends on the environment provided by neighboring, non-stem cells. The stem cell "niche" is the *in vivo* microenvironment where stem cells reside and receive stimuli that determine their fate (Lane et al., 2014). The key components of the niche are direct interactions between stem cells and neighboring cells, secreted factors, inflammation and scarring, extracellular matrix (ECM), physical parameters such as shear stress and tissue stiffness, and environmental signals such as hypoxia. Heterologous cell–cell interactions are invariably present and often exhibit complex, bidirectional signaling dependent on tight regulation and often cell–cell contact. Stem cell niches contain both tissue-specific and seemingly generic cell populations that have specialized roles in each context (Kunisaki et al., 2013, Lo Celso et al., 2009, Tavazoie et al., 2008). Therefore,

the stem cell niche can be targeted using any approach that modulates individual or multiple components of the niche to facilitate regeneration and tissue repair by activating or otherwise manipulating normal stem cell function (Figure 1).

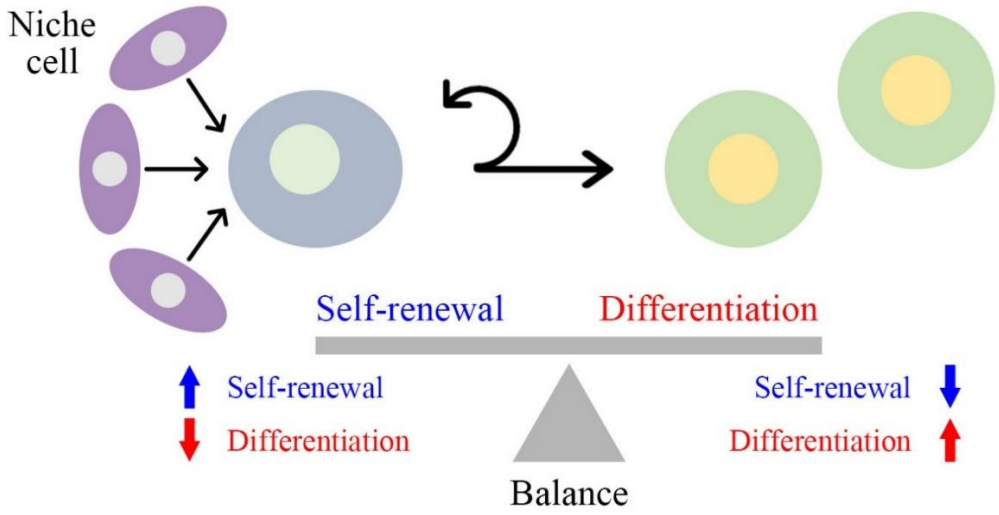

Figure 1. Niche cells controlling the self-renewal of stem cells

A stem cell generates one daughter cell with a stem cell fate (self-renewal) and another daughter cell that differentiates (differentiation). Stem cells can self-renew to maintain the resident stem cell population. The ability of stem cells to undergo self-renewal and retain their identity depends on the environment provided by neighboring non-stem cells, namely, niche cells.

2. Cell cycle

2.1 Cell cycle progression and cyclin-CDK complexes

The cell cycle is a series of events that occur in a cell as it grows and divides. This cycle is divided into four distinct phases: S, M, G1, and G2 phases. In the S phase, chromosomes replicate, while in the M phase, chromosomes undergo transmission. In G1 and G2 or the gap phases, the S phase is temporally separated from the M phase (White & Dalton, 2005). Depending on the mitogenic environment, cells crossing the G1 phase either activate cell division or enter a quiescent G0 state (Liu et al., 2019). The cell cycle in the G1 phase is controlled by an event known as the restriction point. Once this restriction point is crossed, mammalian cells commit proliferation and implement a round of DNA replication after the G1–S transition (Kar, 2016).

A cell decides whether it should enter the cell cycle and divide based on stimulatory and inhibitory messages it receives. Dynamic changes in gene expression as a function of cell cycle progression are regulated by activities between specific cyclins and cyclin-dependent kinases (CDKs) (Bertoli et al., 2013). CDKs are families of protein kinases discovered for their role in regulating the cell cycle. By definition, a CDK binds to a regulatory protein, i.e., a cyclin. Without cyclin, CDK has a limited kinase activity; only the cyclin–

CDK complex is an active kinase, but its activity can be further modulated by phosphorylation and other binding proteins (Morgan, 2007).

Upon mitosis, quiescent cells can re-enter the cell cycle when they are stimulated by mitogenic factors, such as CDK4 and CDK6, to drive the cell cycle progression into the G1 phase. The activity of CDK4/6 is positively controlled by its association with D-type cyclins (cyclin D1, cyclin D2, and cyclin D3) (Malumbres & Barbacid, 2001). During the late G1 phase, the CCNE/CDK2 active complex modulates the retinoblastoma protein to override the restriction point of the G1/S phase at the boundary; as a result, the S phase is initiated (Watanabe et al., 1995). The cyclin A/CDK2 complex terminates the S phase by phosphorylating CDC6 and E2F1; then, this complex drives the cell cycle transition from the S phase to the G2 phase. Subsequently, cyclin A activates CDK1, causing the cells to enter the transition to the M phase. Upon mitosis, CDK1 activity is maintained by the cyclin B/CDK1 complex (Gavet & Pines, 2010) (Figure 2).

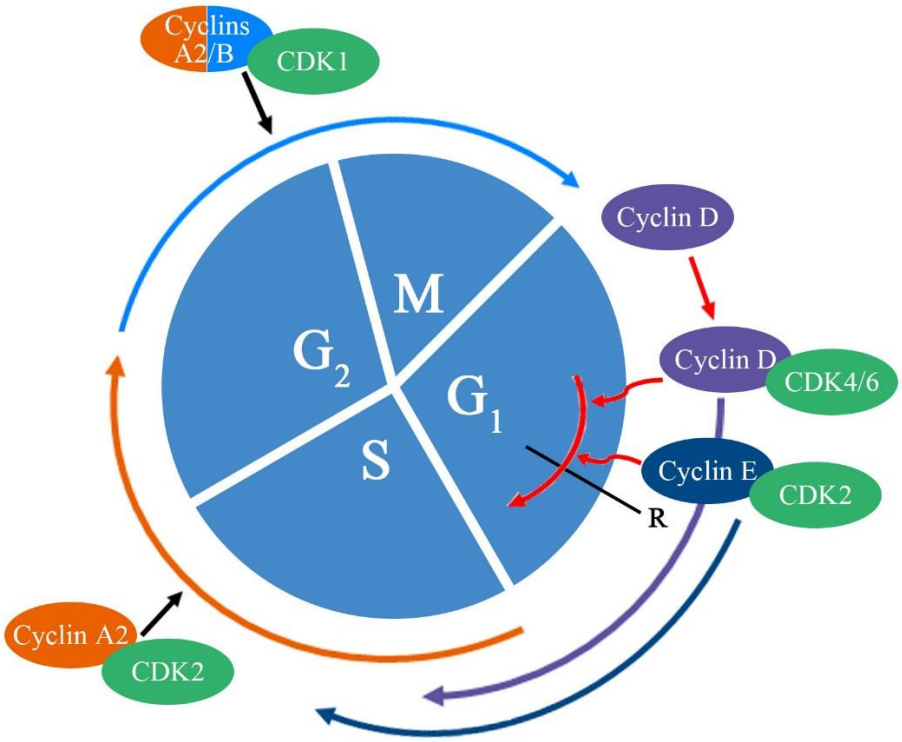

Figure 2. Cell cycle progression and cyclin–CDK complexes

The cell cycle is a series of events that occur in a cell as it grows and divides. The S phase is the period of chromosome replication, and the M phase is the period of chromosome transmission. G1 and G2 act as gap phases that temporally separate the S phase from the M phase. Dynamic changes in gene expression as a function of cell cycle progression are regulated by activities between specific cyclins and cyclin-dependent kinases (CDKs).

2.2 Cell cycle controlling stem cell self-renewal

Self-renewal is division with maintenance of the undifferentiated state. It requires cell cycle control and often maintenance of multipotency or pluripotency depending on the stem cell. Cell cycle control and stem cell self-renewal are closely related processes. As development proceeds, the overall rate of cell cycle progression (which is mainly attributed to the lengthening of the G1 phase) gradually declines as more restricted cell fates in committed progenitors are acquired; ultimately, this process culminates in complete cell cycle withdrawal as post-mitotic cells are generated (Lim & Kaldis, 2013).

Positive regulators of cell cycle progression can either activate self-renewal factors or inhibit differentiation factors to maintain stemness. CDK1 was reported to pairs with OCT4 (POU5F1), a transcription factor crucial for the establishment of pluripotency in ES cells, to repress the caudal type homeobox 2 (CDX2) expression and prevent differentiation into the trophectoderm lineage (Li et al., 2012b). In neural stem cells (NSCs), CDK activity is required for the multisite phosphorylation of Neurogenin 2, a proneural bHLH transcription factor; it inhibits the expression of neurogenic genes (Ali et al., 2011). By contrast, the negative regulators of cell cycle progression activate differentiation factors or inhibit self-renewal factors to induce differentiation. For example, the

binding of p21 and p27 to the enhancer of *Sox2*, which encodes a high mobility group box transcription factor essential for the maintenance of stem cell identity, is key to its transcriptional silencing; thus, differentiation can be initiated in NSCs and ES cells (Li et al., 2012a, Marqués-Torrejón et al., 2013). Although the extensive involvement of CDKs, cyclins, and CDK inhibitors has been investigated, further studies on various stem cells should be performed to specify the cell fate.

3. Spermatogenesis

Spermatogenesis is a complex and cyclic process involving spermatogonial stem cell (SSC) differentiation, meiotic cell division, and sperm production (Chen et al., 2005). Seminiferous tubules in the testes are lined by a complex stratified epithelium containing two distinct populations of cells: spermatogenic cells that develop into spermatozoa and Sertoli cells (SCs) that mainly support and nourish spermatogenic cell lineage and strongly affect the male reproductive capacity (Amiri et al., 2022). Leydig cells are interstitial cells located adjacent to the seminiferous tubules in the testes, and they synthesize testosterone for promoting spermatogenesis and secondary sexual characteristics (Tsai et al., 2023). SSCs continuously maintain not only spermatogenesis via self-renewal to replenish themselves but also differentiation to generates sperms (Chen & Liu, 2015) (Figure 3).

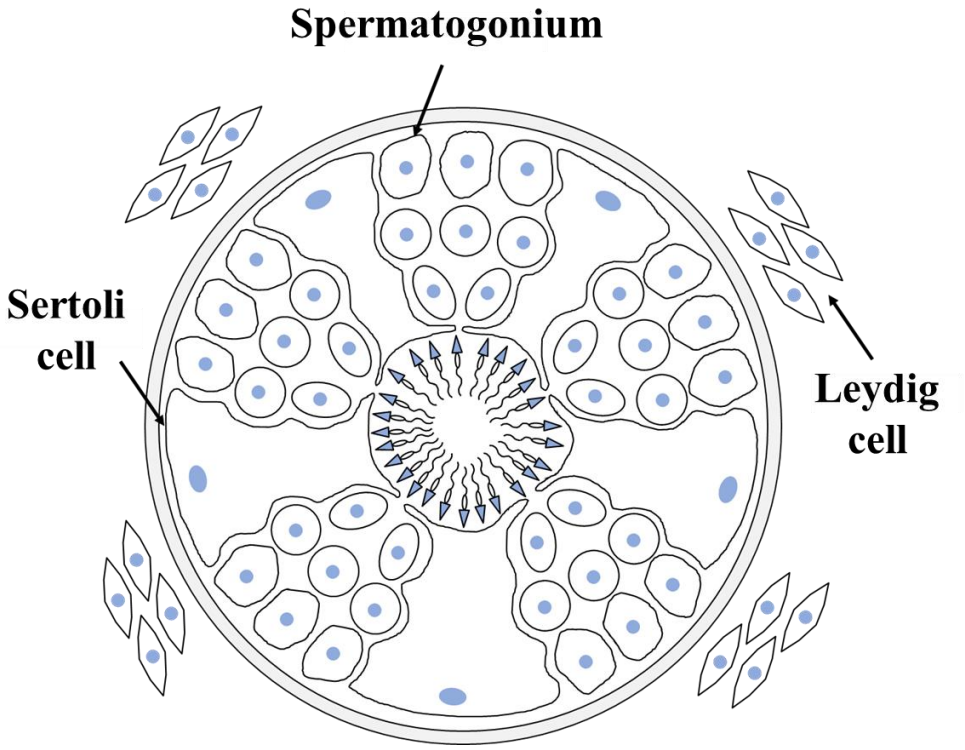

Figure 3. Structure of seminiferous tubules and spermatogenesis

Spermatogenesis occurs in seminiferous tubules lined by a complex stratified epithelium containing a spermatogonium and Sertoli cells. A spermatogonium maintains self-renewal and differentiation to generate sperms. Sertoli cells are the only somatic cells that secrete various spermatogenic factors. Leydig cells are interstitial cells that produce androgen and testosterone.

3.1 Testis development

In mammals, the ovary and testes are derived from a common precursor structure, namely, the bipotential gonad (Endo et al., 2019). In mice, the development of the bipotential gonad begins on embryonic day (E) 10.0 and continues until E11.5–E12.0. PGCs migrate to the somatic gonad, where they undergo gametogenesis to ultimately produce oocytes or sperms depending on their location (in an ovary in females or a testes in males. Differences between the somatic cellular composition of the ovaries and testes are microscopically evident by E12.5. However, germ cells remain morphologically indistinguishable between the sexes until E13.5. Subsequently, female germ cells enter meiotic prophase I and begin to differentiate as oocytes; male germ cells remain mitotically active and later arrest in the G0/G1 phase of the mitotic cell cycle (Endo et al., 2019, Hu et al., 2013).

SSCs are considered single cells located at the basement membrane of seminiferous tubules. In rodents, these cells are called A single (A_s) spermatogonia that regularly undergo mitotic divisions. SSCs give rise to spermatogonia, thereby supporting daily sperm production. Undifferentiated diploid spermatogonia undergo differentiation and further rounds of division to produce spermatocytes, which enter the meiotic process (De Rooij, 2017). A_s

spermatogonia divide and give rise to two paired (A_{pr}) spermatogonia, and then 4-32 aligned (A_{al}) spermatogonia are connected to each other (Song & Wilkinson, 2014). During puberty, the testis undergoes dramatic developmental and structural changes, including the proliferation and maturation of Sertoli cells and the beginning of spermatogenesis (Guo et al., 2020).

3.2 Meiosis

Meiosis is essential for the production of haploid gametes from spermatocytes and the maintenance of genome integrity (Li et al., 2005). Prophase of meiosis I is unique because it is elongated and further divided into leptotene, zygotene, pachytene, diplotene, and diakinesis. During these prophase I substages, DNA double-strand breaks, homologs align and undergo synapsis, and crossover forms to ensure homologous recombination between non-sister chromatids (Pawlowski & Cande, 2005). Meiosis is precisely controlled by intrinsic and extrinsic factors, as shown in numerous gene KO studies.

4. SSC self-renewal

4.1 SSCs

To maintain themselves, SSCs produce essential proteins, including promyelocytic leukemia zinc finger (PLZF), ID4, and paired box protein 7 (PAX7) (Aloisio et al., 2014, Lovelace et al., 2016, Sun et al., 2015). The expression of ID4 is selective for A_s spermatogonia, and the level of ID4 is predictive of stem cell or progenitor capacity in spermatogonia; it also dictates the interface of transition between different functional states (Helsel et al., 2017, Sun et al., 2015). PAX7 is highly expressed in $CD49f^+$ SSCs in several species, and PAX7 can maintain the self-renewal of SSCs (Aloisio et al., 2014, Du et al., 2021). PLZF protein belongs to the Krüppel-like zinc finger protein family, which regulates of diverse cellular processes, including cell proliferation, apoptosis, differentiation, and development (Pearson et al., 2008). PLZF was the first transcription factor identified to be involved in SSC self-renewal (Costoya et al., 2004). PLZF is required autonomously to maintain SSCs and is antagonized by SALL4 during differentiation (Hobbs et al., 2012).

4.2 Sertoli cells

The self-renewal and differentiation of SSCs are strictly controlled by a special microenvironment in seminiferous tubules. Fibroblast growth factor (FGF) signaling regulates SSC self-renewal and male germline development. FGF2 is produced by Sertoli cells, Leydig cells, and differentiating germ cells in the testes (Chen & Liu, 2015). It is involved in spermatogonial proliferation (Zhang et al., 2012). Glial cell line-derived neurotrophic factor (GDNF) is secreted by Sertoli cells. The stage-specific ectopic expression of GDNF causes a $GFRA1^{+}$ $LIN28^{-}$ SSC population to accumulate, thereby enhancing SSC activity. This phenomenon implies that GDNF normally limits self-renewal to specific stages (Sharma & Braun, 2018). ETS variant 5 (ETV5; also known as ERM) is also a protein critical for the maintenance of stem/progenitor spermatogonia within Sertoli cells (Chen et al., 2005). Many ETS transcription factors are regulated by FGF signaling in Sertoli cells (Ishii et al., 2012) (Figure 4).

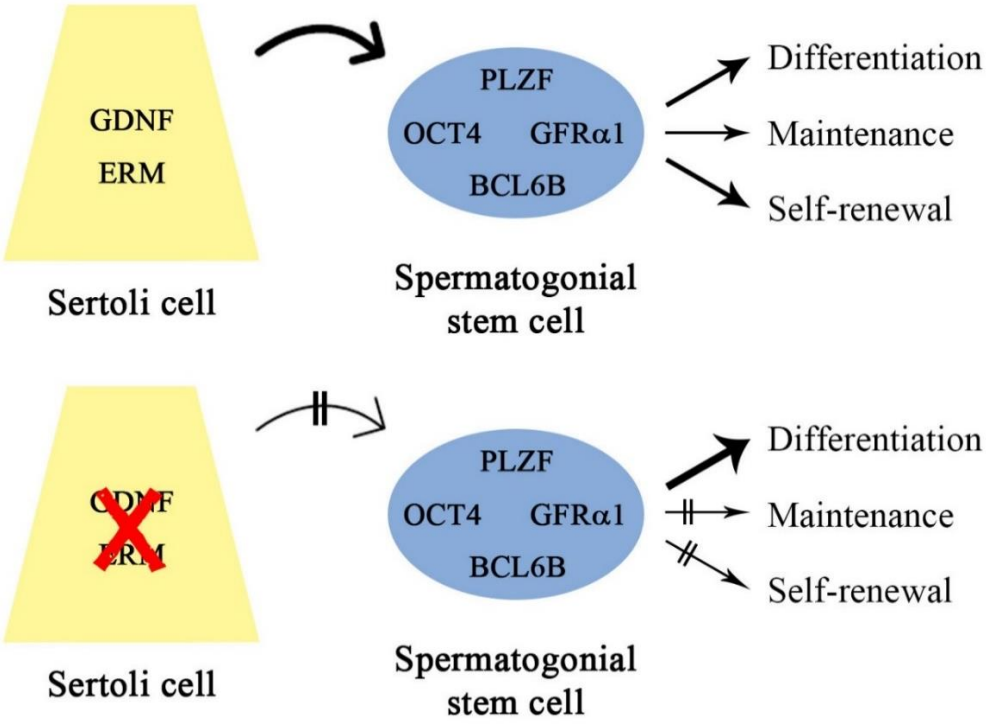

Figure 4. Sertoli cell–Spermatogonial stem cell interaction on self-renewal and differentiation

Spermatogonial stem cells (SSCs) undergo spermatogenesis while maintaining a good balance between self-renewal and differentiation. They produce most proteins that regulate their self-renewal. However, GDNF and ERM, which are proteins produced by Sertoli cells, also transmit signals to SSCs to regulate self-renewal. If these genes are deleted, self-renewal does not occur, and only differentiation occurs; consequently, the stem cell pool is not maintained.

4.3 Sertoli cell-only (SCO) syndrome

The imbalance between the self-renewal and differentiation of SSCs completely disrupts spermatogenesis; when imbalance occurs, Sertoli cell-only (SCO) syndrome becomes initiated and progresses (Chen et al., 2022). SCO syndrome, including infertility, refers to the dysfunction of the male reproductive system. The testes of males with SCO syndrome are typically characterized by Sertoli cells instead of spermatogenic cells lining the seminiferous tubules; they are also characterized by markedly atrophied seminiferous tubules with thickened tubule walls. In rare cases of SCO syndrome, very few segments of seminiferous tubules are dilated and capable of producing spermatozoa (Dabaja & Schlegel, 2013). Therefore, the self-renewal of SSCs must be accurate to prevent SCO syndrome.

5. Microtubule-associated serine/threonine kinase family member 4 (MAST4)

Microtubule-associated serine/threonine kinase family member 4 (MAST4) of the protein kinase superfamily contains the following highly conserved domains: the domain of unknown function (DUF), the catalytic domain of the protein serine/threonine kinase, and the postsynaptic density protein 95 (PSD95), discs large MAGUK scaffold protein 1 (DLG1), and zona occludens 1 (ZO-1) (PDZ) domain (Sun et al., 2006). Since MAST4 was identified in 2006, its expression has been investigated in the brain and its interaction with several proteins as a kinase (Garland et al., 2008, Gongol et al., 2017). However, the fundamental role of MAST4 in stem cells during vertebrate development remains unclear.

6. Aim of this study

This study aims to determine how MAST4 fundamentally regulates the SSC self-renewal during spermatogenesis and the role of MAST4 in the cell cycle of SSCs.

1) To examine the expression pattern of MAST4 during spermatogenesis

2) To investigate the MAST4–ERM interaction for SSC self-renewal

3) To determine how MAST4 regulates the cell cycle of SSCs

II. MATERIALS AND METHODS

All experiments were approved by Yonsei University College of Dentistry, Intramural Animal Use and Care Committee and they were performed in accordance with the guidelines of this committee.

1. Animals

Mice were housed in a temperature-controlled room (22°C) under artificial illumination with a 12-hour light/dark cycle and 55% relative humidity, and they had ad libitum access to food and water. Mice from postnatal day 1 (PN 1D), postnatal week 3 (PN 3W), PN 6W, PN 22W and postnatal month 21 (PN 21M) were used in this study. All the operational procedures were performed under deep anesthesia.

To generate *Mast4* KO mice by CRISPR/Cas9-mediated gene targeting, we targeted exon 1 and exon 15 of *Mast4* (RefSeq Accession number: 175171); 5'-GGAAACTCTGTCGGAGGAAG-3' (exon 1) and 5'-GGCACAAAGAGTCCCGCCAG-3' (exon 15). We then inserted each sequence into the pX330 plasmid, which carried both guide RNA and Cas9 expression units, from Dr. Feng Zhang (Addgene plasmid 42230) (Cong et al., 2013). We named these vectors pX330-

Mast4-E1 and pX330-*Mast4*-E15. The pregnant mare serum gonadotropin (5 units) and the human chorionic gonadotropin (5 units) were intraperitoneally injected into female C57BL/6J mice (Charles River Laboratories, Kanagawa, Japan) at 48 h interval, which were then mated with male C57BL/6J mice. The pX330-*Mast4*-E1 and pX330-*Mast4*-E15 (circular, 5 ng/μl each) were co-microinjected into 231 zygotes collected from oviducts of the mated female mice. The surviving 225 injected zygotes were transferred into oviducts in pseudopregnant ICR females, and 47 newborns were obtained. We collected genomic DNA from the tails of 31 founder mice that survived. To confirm the indel mutation induced by CRISPR/Cas9, we amplified the genomic region, including the target sites by PCR with the primers for exon 1 target (*Mast4*-1 genotype F: 5'-GTAGGGACTCCACGCTCCAG-3' and *Mast4*-1 genotype R: 5'-CCGGACCCTAGTCTCTTCG-3') and for exon 15 target (*Mast4*-15 genotype F: 5'-GGGTTCTCTGCGAAAGTCAG-3' and *Mast4*-15 genotype R: 5'-ATCCCTGTGTTCCGTTTCAG-3'). The PCR products were sequenced by using BigDye Terminator v3.1 Cycle Sequencing Kit (Thermo Fisher Scientific, MA, USA), *Mast4*-1 genotype F primer and *Mast4*-15 genotype F primer. In male founder #38, we found indel mutations in both exon 1 and exon 15 without pX330 random integration. To identify the indel sequence and whether indel mutations in exon 1 and exon 15 occurred on the same chromosome (cis manner),

the founder #38 was mated with a wild-type female and the indel mutations in F1 were sequenced. We obtained 17 F1 newborns, and 12 of them carried 71 bp deletion (chr13:103,333,981-103,334,051: GRCm38/mm10) in exon 1 and 3 bp deletion (chr13:102,774,360-102,774,362) in exon 15 in a cis manner. The deletion in exon 1 produces a frameshift so that translation stops at exon 1 (Figure 5).

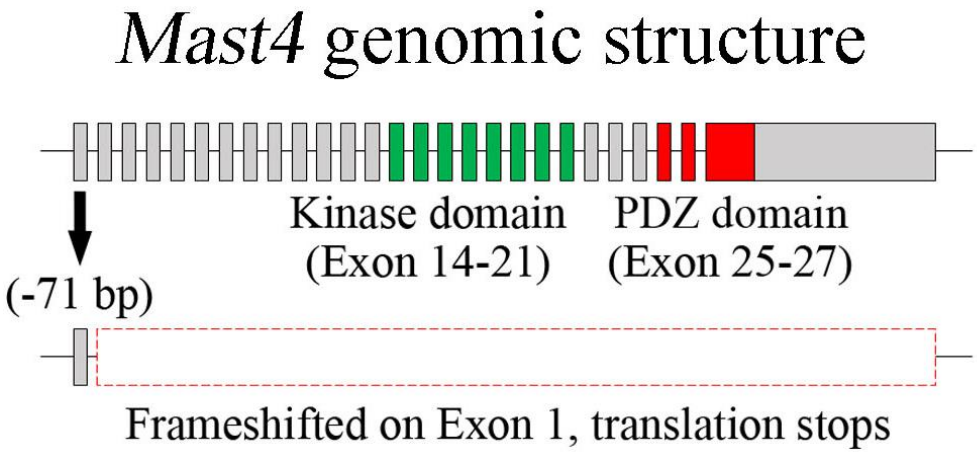

Figure 5. *Mast4* genomic structure and the generation of *Mast4* KO mice

Microtubule associated serine threonine kinase family member 4 (*Mast4*) has a kinase domain and a PDZ domain. To delete *Mast4*, the CRISPR/Cas9 system was used to carry 71 bp deletion and create a frameshift in exon 1 of the *Mast4* gene, preventing translation of MAST4.

2. Histology

2.1 Wax section

All wax blocks were sectioned serially in 4 μm thickness with microtome (RM2235, Leica, Germany). They were mounted on slides coated with poly-L-lysine (Muto Pure Chemicals, Japan) and dried on slide warmer at 37°C overnight.

2.2 Hematoxylin and Eosin (HE)

Melt wax on slide at 60°C for 15 minutes for staining. Then the slides were washing in xylene. Rehydrate through sequential alcohols from 100% to 70% and washing in running tap water. Slides were stained in Harris hematoxylin for a minute and washed in running tap water. Dipping slides to 0.5% concentrated HCl in 70% alcohol then washing in running tap water. 2 or 3 times dipping in 1% ammonia solution and washing in running tap water. Slides were stained in eosin for 15 seconds then washed in running tap water. Dehydrate through sequential alcohols from 70% to 100%. Slides were washed in xylene 2 times for 5 minutes each. Cover glasses were mounted.

3. Immunohistochemistry (IHC)

Staining was performed on 4 μm paraffin embedded sections. After deparaffinization, the slides were boiled in 10 mM citrate buffer (pH 6.0) for 20 min and cooled at room temperature for 20 min. The specimens were incubated with primary antibodies at 4°C overnight. Primary antibodies are listed in Table 1. The specimens were incubated with Alexa Fluor secondary antibodies (Invitrogen, OR, USA) for 2 h at room temperature and were counterstained with TO-PRO™-3 (T3605, Invitrogen, OR, USA; 1:1000) or DAPI (D1306, Invitrogen, OR, USA; 1:1000). The sections were examined using a confocal laser microscope (TCS SP8, Leica, Germany).

Name	Catalog No.	Source	Dilution
MAST4	BS5791	Bioworld Technology, Inc.	1:150
SOX9	14-9765-80	Invitrogen	1:200
AMH	SC-166752	Santa Cruz Biotechnology, Inc.	1:100
3β-HSD	SC-515120	Santa Cruz Biotechnology, Inc.	1:100
DDX4	ab13840	Abcam	1:100
ERM	ab102010	Abcam	1:200
PCNA	ab29	Abcam	1:200
PLZF	SC-28319	Santa Cruz Biotechnology, Inc.	1:200
c-Kit	ab231780	Abcam	1:100
CDK2	SC-6248	Santa Cruz Biotechnology, Inc.	1:100
p21	SC-397	Santa Cruz Biotechnology, Inc.	1:100
	ab107099	Abcam	1:100
p53	ab26	Abcam	1:100

Table 1. Primary antibodies for Immunohistochemistry

4. Section *in situ* hybridization

The sections were baked at 60°C, de-waxed in xylene, rehydrated through a graded series of alcohol washes and post-fixed in 4% PFA. The sections were prehybridized in a humid chamber containing 50% formamide in 2×SSC at 55°C for 30 min. Digoxigenin (DIG)-labeled RNA probes were pre-warmed at 85°C and hybridized to the sections overnight at 65°C. At least 10 specimens were examined in each stage. The primer sequences of the *Mast4* probe are as follows:

Mast4-F: 5′-CAA AAG GCA AAG AGC CTG TC-3′; R: 5′-TGC GTC TGT GCA TTT CTT TC-3′.

5. 5'-iodo-2'-deoxyuridine (IdU)/5'-bromo-2'-deoxyuridine (BrdU) injection and cell cycle time (T_c) calculation

Both IdU and BrdU were injected into the mice (100 mg/kg). Testes were embedded in paraffin and serially sectioned into 4 μm slices. The specimens were incubated with anti-PLZF (SC-28319, Santa Cruz Biotechnology, Inc., USA; 1:200) to label spermatogonial stem cells in serial sections. In addition, the specimens were incubated with anti-BrdU (#347580, BD Biosciences, USA; 1:100), which recognizes both IdU and BrdU, and anti-BrdU (ab6326, Abcam,

UK; 1:200) for double staining. T_c was calculated using the ratio of IdU-only-labeled cells (leaving cells, L_{cells}) and PLZF-labeled cells (the total number of SSCs, P_{cells}) (Martynoga et al., 2005, Quinn et al., 2007). Cells labeled with IdU only left the S phase during the interval time (12 h) between the IdU and BrdU injections (Figure 6). Therefore, the following formula can be used to calculate T_c:

$$\frac{T_c}{Interval\ time} = \frac{P_{cells}}{L_{cells}} \text{ or } T_c = \frac{P_{cells}}{L_{cells}}\ x\ interval\ time$$

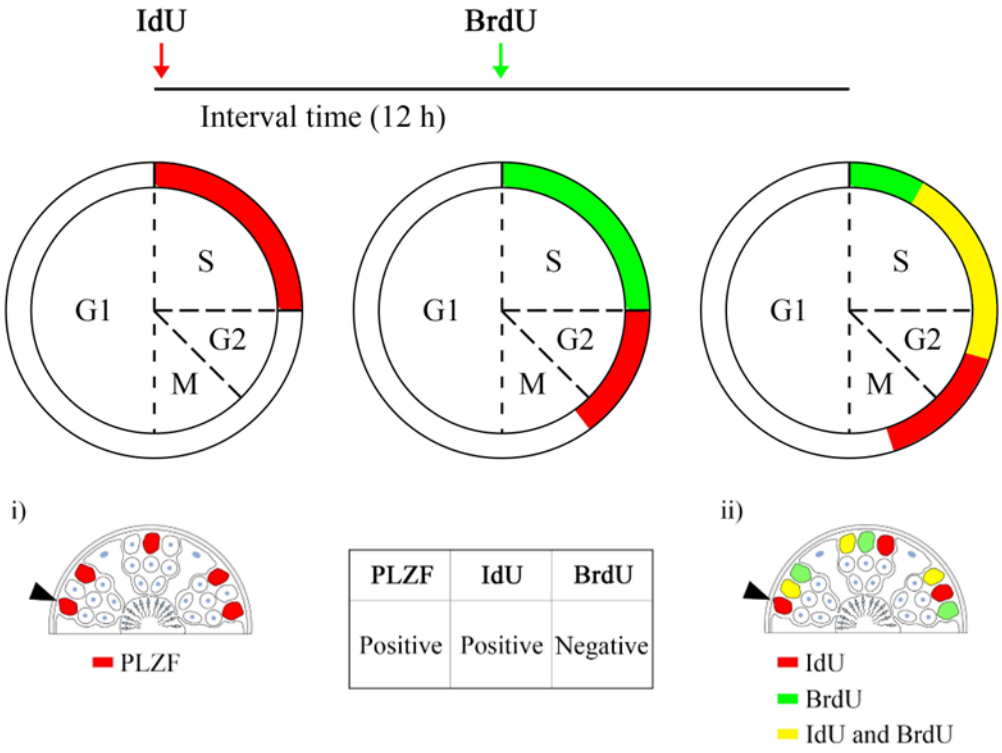

PLZF	IdU	BrdU
Positive	Positive	Negative

$T_c = P_{cells} / L_{cells}$ x interval time (h)

- P_{cells} = PLZF-expressing cells
- L_{cells} = Leaving cells (IdU only-labeled cells)

IdU only-labeled cell
BrdU only-labeled cell
IdU- & BrdU-labeled cell

Figure 6. IdU/BrdU injection for cell cycle calculation

To estimate cell cycle time, the mice are injected with IdU at T = 0 h to label all cells in S phase at the beginning of the experiment. At T = 12 h, an injection of BrdU is given and the testes are fixed after 0.5 h, sufficient to label the S fraction at the end of the labeling period. During the 12 h interval when cells are exposed to IdU but not BrdU, some cells of the initial S phase will leave S-phase and consequently will be labeled just with IdU; this is the leaving fraction (L_{cells}). (i) PLZF-positive cells were counted per unit area (P_{cells}, arrowhead). (ii) In adjacent serial sectioning, IdU-only labelled cells were counted under co-localization with PLZF (L_{cells}, arrowhead). Tc was calculated using the formula in Figure 6. By staining tissue sections with antibodies that allow to distinguish cells labeled with just IdU from those which incorporated BrdU and IdU, we can count the L_{cells} fractions.

6. Testis tissue culture

Testes from PN 1D WT and *Mast4* KO male mice were decapsulated and gently fragmented into several pieces 1–3 mm in diameter. Explants of testes were cultured as modified from the methods described by Sato et al. (Sato et al., 2011). The tissues were placed in a Trowell-type organ culture and incubated with RPMI medium 1640 (#11875-093, Life Technologies, USA) supplemented with 10% knockout serum replacement (#10828-010, Life Technologies, USA), 100 units/ml of penicillin, and 100 μg/ml of streptomycin at 37°C in 5% CO2. The medium was added to bFGF (#100-18B; PeproTech, Inc., USA) and CXCL12 (460-SD-010; R&D Systems, Inc., USA) (100 ng/ml final) or vehicle (Figure 7). The culture medium was replaced every two days. Explants of testes were collected one week later and fixed in 4% paraformaldehyde or harvested using TRIzol® reagent.

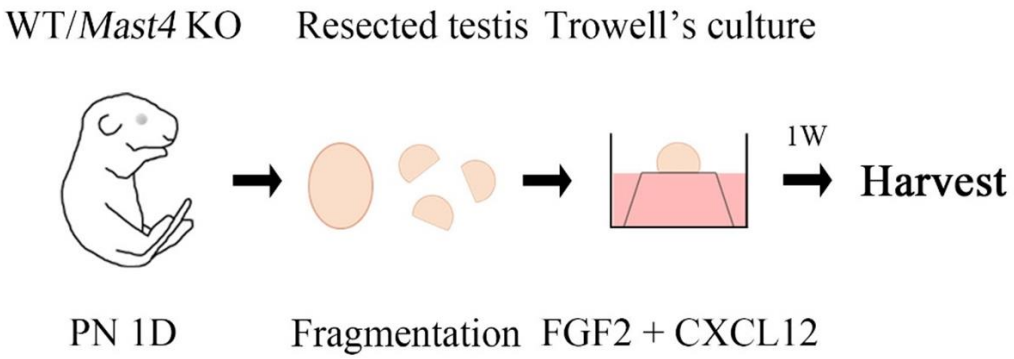

Figure 7. *In vitro* culture of mouse testis tissue using Trowell's culture

The outer layer of testis, tunica albuginea, was removed and fragmented using the Trowell's culture technique, and culture was performed using two proteins, FGF2 and CXCL12, which are upstream and downstream of MAST4.

7. Cell culture and lentivirus transduction

TM4 (ATCC® CRL-1715™, USA) cells, mouse Sertoli cell line, were cultured in DMEM/F-12 (#11320-033, Life Technologies, USA) supplemented with 2.5% fetal bovine serum and 5% horse serum at 37°C in a humidified atmosphere with 5% CO2.

LentiCRISPRv2 vector (#52961, Addgene, USA) was digested with BsmBI and ligated with annealed oligonucleotide targeting *Mast4* exon 1, 5'-TACCCTGCCGCTGCCGCACC-3' (LentiCRISPRv2-*Mast4* Ex1). The vector without insertion was used as a control. To generate the lentivirus, HEK293T cells were transfected with LentiCRISPRv2-*Mast4* Ex1 and packaging vectors (pVSVG and psPAX2) using FuGENE at 70% confluency. The viral supernatant was harvested at 48 h post-transfection, filtered through 0.45-μm filters and applied to TM4 cells. The clonal cells were selected with puromycin (A11138-03, Life Technologies, USA) at 48 h post-transfection.

To manipulate FGF signaling, cells were cultured in media containing 50 ng/ml FGF2 for 3, 6, 12, 24 h and 10 μM SU5402 (SML0443, Sigma-Aldrich, USA) for 24 h. SU5402 was dissolved in dimethyl sulfoxide vehicle (DMSO; D2650, Sigma-Aldrich, USA).

8. Protein extraction, nuclear/cytoplasmic fractionation and western blot

Nuclear and cytoplasmic fractions of TM4 cells were prepared using the NE-PER Nuclear and Cytoplasmic Extraction reagents (Thermo Scientific). Cell extracts were fractionated by SDS-PAGE transferred to a polyvinylidene difluoride (PVDF) membrane using a transfer apparatus (Bio-Rad). After incubation with 5% skim milk in TBST (10 mM Tris, pH 7.4, 150 mM NaCl, 0.1% Tween 20) for 60 min, the membrane was incubated with primary antibodies at 4°C overnight. Primary antibodies are listed in Table 2. Membranes were washed six times for 10 min and incubated with HRP-conjugated secondary antibodies for 2 h. Blots were washed six times with TBST and developed with the ECL system (RPN2232, GE Healthcare Life Sciences, USA).

Name	Catalog No.	Source	Dilution
MAST4	PA5-36976	ThermoFisher	1:500
ERM	ab102010	Abcam	1:1000
PLZF	SC-28319	Santa Cruz Biotechnology, Inc.	1:100
CDK2	SC-6248	Santa Cruz Biotechnology, Inc.	1:1000
p21	SC-6246	Santa Cruz Biotechnology, Inc.	1:200
p53	SC-126	Santa Cruz Biotechnology, Inc.	1:200
Lamin B	SC-374015	Santa Cruz Biotechnology, Inc.	1:1000
GAPDH	SC-32233	Santa Cruz Biotechnology, Inc.	1:1000
α-tubulin	T6199	Sigma-Aldrich	1:1500

Table 2. Primary antibodies for Western blot

9. Immunoprecipitation (IP)

Cells were lysed in a RIPA buffer containing a protease inhibitor cocktail (cOmplete™; #11697498001, Roche, IN, USA). Cell extracts were incubated with the indicated primary antibodies overnight at 4°C. Antibody-bound proteins were precipitated with Dynabeads™ Protein G (Invitrogen). Samples were separated by SDS-PAGE, followed by electrotransfer to PVDF membrane. The membrane was blocked for 1h at room temperature and incubated overnight at 4°C with the primary antibody. The primary antibodies are listed in Table 3. Membranes were washed three times with TBST and incubated with HRP-conjugated secondary antibodies for 2 h. Blots were washed three times with TBST and developed with the ECL system (RPN2232, GE Healthcare Life Sciences, USA).

Name	Catalog No.	Source	Dilution
GST	SC-138	Santa Cruz Biotechnology, Inc.	1:1000
HA	SC-805	Santa Cruz Biotechnology, Inc.	1:1000
	SC-7392	Santa Cruz Biotechnology, Inc.	1:1000
p-Serine	P5747	Sigma-Aldrich	1:1000
β-actin	A5441	Sigma-Aldrich	1:4000
FLAG	F3165	Sigma-Aldrich	1:4000
	SC-166355	Santa Cruz Biotechnology, Inc.	1:1000
GAPDH	SC-32233	Santa Cruz Biotechnology, Inc.	1:1000

Table 3. Primary antibodies for Immunoprecipitation

10. RNA preparation, reverse transcription-polymerase chain reaction (RT-PCR) and real time-quantitative polymerase chain reaction (RT-qPCR) analysis

10.1 RNA preparation

The total RNA was extracted using TRIzol® reagent (#15596-026, Thermo Fisher Scientific, USA). Testis tissues and cell lysates were and homogenized in 1 ml of TRIzol reagent. 0.2 ml of chloroform was added and incubated for 3 minutes. Then the samples were centrifuged for 20 minutes at 13,000 g at 4°C. Upper colorless aqueous phase was transferred to new tubes with avoiding transferring of interphase. Then, same amount of isopropanol was added to the aqueous phase and incubated at -80°C for overnight. The samples were centrifuged for 20 minutes at 13,000 g at 4°C. The supernatant was discarded. The pellet was resuspended in 1 ml of 70% EtOH and vortexed briefly for washing, then centrifuged for 20 minutes at 13,000 g at 4°C. The supernatant was discarded and the RNA pellet was air dried. The RNA was resuspended in 40 μl of RNase-free water.

10.2 Reverse Transcription

The cDNA library was generated from total RNA using the Maxime™ RT PreMix Kit (#25081, iNtRON Biotechnology, Korea). Into the kit, 1 μg of total RNA and RNase-free water (up to 20 μl) were added and incubated in Thermal Cycler Dice TP600 (Takara, Japan) at 45°C for 1 hour, then 95°C for 5 minutes for inactivation of reverse transcriptase.

10.3 RT-PCR

RT-PCR was performed using the Thermal Cycler Dice TP600 (Takara, Japan) with AccuPower® PCR PreMix (Bioneer, Korea). The amplification programme consisted of 40 cycles of the following: denaturation at 95°C for 300 seconds, annealing at 60°C for 30 seconds and extension at 72°C for 60 seconds. The expression levels of each gene are expressed as normalized ratios against the *Gapdh* housekeeping gene. The oligonucleotide RT-PCR primers listed in Table 4.

10.4 RT-qPCR

RT-qPCR was performed using a StepOnePlus Real-Time PCR System (Applied BioSystems, USA). The amplification program consisted of 40 cycles of denaturation at 95°C for 15 s and annealing at 61°C for 60 s. The RT-qPCR

analysis of each sample was performed in triplicate. The expression levels of each gene are expressed as normalized ratios against the *B2m* housekeeping gene. The oligonucleotide RT-qPCR primers are listed in Table 4.

Gene	Sequence (5'-3')
[RT-PCR]	
Mast4	F: 5’- CAA AAG GCA AAG AGC CTG TC-3’
	R: 5’- TGC GTC TGT GCA TTT CTT TC-3’
Erm	F: 5’-CCG AGT TGT CGT CCT GTA G-3’
	R: 5’-ACT GGC TTT CAG GCA TCA TC-3’
Cxcl5	F: 5’-GAA AGC TAA GCG GAA TGC AC-3’
	R: 5’-GGT CCC CAT TTC ATG AGA GA-3’
Cxcl12	F: 5’-TTT CAC TCT CGG TCC ACC TC-3’
	R: 5’-TAA TTT CGG GTC AAT GCA CA-3’
Ccl12	F: 5’-TCC TCA GGT ATT GGC TGG AC-3’
	R: 5’-GGG AAC TTC AGG GGG AAA TA-3’
Gapdh	F: 5’-ACT CCA CTC ACG GCA AAT TC-3’
	R: 5’-CCT TCC ACA ATG CCA AAG TT-3’
[RT-qPCR]	
Mast4	F: 5’-AGG AAG TCC CGC ATA CCA GG-3’
	R: 5’-TCC CAC TCT TCA GCA GGA GC-3’
Erm	F: 5’-GCA GGA GGC TTG GTT AGC TG-3’
	R: 5’-CGT GGC TAC AGG ACG ACA AC-3’
p21	F: 5’-TTC CGC ACA GGA GCA AAG TG-3’
	R: 5’-TCC CAG ACG AAG TTG CCC T-3’
Ccna2	F: 5’-GAG ACC CTG CAT TTG GCT GT-3’
	R: 5’-ATA GCA GCC GTG CCT ACA AG-3’
p53	F: 5’-ATG AAC CGC CGA CCT ATC CT-3’
	R: 5’-GCA GTT CAG GGC AAA GGA CT-3’
B2m	F: 5’-CCT GGT CTT TCT GGT GCT TG-3’
	R: 5’-CCG TTC TTC AGC ATT TGG AT-3’

F, forward primer; R, reverse primer

Table 4. Primers for RT-PCR and RT-qPCR

11. RNA sequencing (RNA-seq) analysis

Libraries were prepared for 150 bp paired-end sequences using a TruSeq Stranded mRNA Sample Preparation Kit (Illumina, CA, USA). Namely, mRNA molecules were purified and fragmented from 1 μg of total RNA using oligo (dT) magnetic beads. The fragmented mRNAs were synthesized as single-stranded cDNAs through random hexamer priming. By applying this as a template for second strand synthesis, double-stranded cDNA was prepared. After the sequential process of end repair, A-tailing and adapter ligation, cDNA libraries were amplified with Polymerase Chain Reaction (PCR). The quality of these cDNA libraries was evaluated with the Agilent 2100 BioAnalyzer (Agilent, CA, USA), and they were quantified with the KAPA library quantification kit (Kapa Biosystems, MA, USA) according to the manufacturer's library quantification protocol. Following cluster amplification of denatured templates, sequencing was progressed as paired-end (2×150bp) using Illumina NovaSeq 6000 sequencer (Illumina, CA, USA). Low quality reads were filtered according to the following criteria: reads contain more than 10% skipped bases (marked as 'N's), reads contain more than 40% of bases whose quality scores are less than 20 and reads with an average quality score of less than 20. The whole filtering process was performed using the in-house scripts. Filtered reads were mapped to the reference genome related to the species using the aligner TopHat23. The

gene expression level was measured with Cufflinks v2.1.124 using the gene annotation database of the species. To improve the accuracy of the measurement, multi-read-correction and frag-bias-correct options were applied. All other options were set to default values.

12. Luciferase assay

The mouse *Cxcl5* (-1127~+122) and *Cxcl12* (-1580~+89) promoter were amplified by PCR from the genomic DNA of TM4 cells and isolated by a HiYieldTM Genomic DNA Mini Kit (Real Genomics). For *Cxcl5* promoter-F: 5'-GAT CAC GCG TTA AGT CCC ACG GAT GAG TCC-3'; R: 5'-GAT CCT CGA GGA GCA CCA GCT CGG GAT A-3' and *Cxcl12* promoter-F: 5'-GAT CAC GCG TGC GCT TGA TCT CGG ATT ACT-3'; R: 5'-GAT CCT CGA GGA GCT GGA CAG CAA GAG GAC-3'. The amplified PCR fragment was cloned into the MluI and XhoI sites of the pGL3 basic vector (Promega). TM4 cells were transfected with *Cxcl5*- and *Cxcl12*-promoter luciferase report plasmids and HA-MAST4 PDZ using polyethylenimine (#24765, Polysciences). Cells were treated with FGF-2 (50 ng/ml for 18 h) (Peprotech). The luciferase activities were analyzed using the Luciferase Assay System Kit (Promega). All

assays were carried out in triplicate, and all values were normalized for transfection efficiency against β-galactosidase activities.

13. Terminal deoxynucleotidyl transferase dUTP nick end labeling (TUNEL) staining

A terminal deoxynucleotidyl transferase dUTP nick end labelling (TUNEL) assay was performed using an *in situ* cell apoptosis detection kit (#4810-30-K, Trevigen, Inc., USA). The 7 μm thick sections were treated with 20 μg/ml proteinase K in 10 mM Tris–HCl, pH 8.0, for 25 min at room temperature. The samples were incubated with the labelling reaction mixture at 37 °C for 1 h and HRP-streptavidin solution for 5 minutes at room temperature. A 3, 3′-diaminobenzidine (DAB) was used as a substrate solution to detect the sites of *in situ* apoptosis. At least five specimens were examined in each experiment.

14. Sperm count

To count sperm, both cauda epididymides from PN 6W mice were collected, dissected and placed in 2 ml of Hanks' Balanced Salt Solution (HBSS; #14025-

092, Life Technologies, USA) for 30 min to allow the release of motile cells (swim-out procedure). The total sperm number from suspension sperm was obtained using a hemocytometer.

15. Statistical analysis

The graphic results were expressed as the mean ± standard deviation (SD). A GraphPad Prism 7 (GraphPad Software, San Diego, CA, USA) was used to analyze the data. Comparison of two groups was performed using an unpaired two-tailed t-test. Comparison of multiple groups was performed by one-way ANOVA or by two-way ANOVA for luciferase assay followed by Tukey's multiple comparisons test. The p value < 0.05 was considered significant.

III. Section I: MAST4 activates ERM in Sertoli cells for SSC self-renewal

1. Introduction

Sertoli cells, the only somatic cell type in seminiferous tubules, directly interact with SSCs to control their proliferation and differentiation by secreting specific factors such as GDNF and ERM. GDNF secreted by Sertoli cells binds to a receptor complex formed by the association of the receptors GDNF family membrane receptor alpha 1 (GFRα1) and rearranged during transfection (RET), which elicit an intracellular response (Nakagawa et al., 2010, Takashima et al., 2015). In the testes, GFRα1 is expressed by A_s and possibly A_{pr} and A_{al} spermatogonia (Nakagawa et al., 2010). In Sertoli cells, ERM regulates the expression of several chemokine-encoding genes such as C-C-motif ligand 9 (*Ccl9*), *Ccl7*, C-X-C-motif ligand 5 (*Cxcl5*, and *Cxcl12* (Chen et al., 2005). The chemokines CCL9 and CXCL12 expressed by Sertoli cells and their cognate receptors, namely, CCR1 and CXCR4 localized in SSCs, play important roles during male germline development (Loveland et al., 2017, Simon et al., 2010).

Mice with a global deletion of *Erm* have the first wave of spermatogenesis, but stem/progenitor spermatogonia are completely lost by day 36 (Schlesser et al., 2008); as a result, a Sertoli cell-only phenotype manifests, and aspermia ultimately occurs in adulthood (Chen et al., 2005). In human SCO syndrome, aberrant gene expression by Sertoli cells may decrease their niche function and contribute to SSC deficiency and dysfunction in infertile men (Paduch et al., 2019a). Furthermore, Sertoli cells express abnormally low levels of GDNF, FGF8, and bone morphogenic protein 4 (BMP4), which are growth factors well characterized as SSC regulators and spermatogonium progenitors in mice (Hasegawa & Saga, 2014, Parker et al., 2014, Yang et al., 2016).

To the best of our knowledge, the identity and role of MAST4 remain largely unexplored during spermatogenesis, especially SSC self-renewal, which is regulated by interactions between Sertoli cells and SSCs. In this section, evidence supporting the existence and role of MAST4 in Sertoli cells is provided.

2. Results

2.1. Spermatogenic dysregulation in *Mast4* KO testes

Studies have monitored the undefined reproduction failure in *Mast4* KO mice, and intensive studies on spermatogenesis have been performed. In the present study, the size of *Mast4* KO testes was reduced (Figure 8A), and the total sperm number was dramatically decreased compared with those of the wild-type (WT) testes (Figure 8B). These results indicated a characteristic of infertility.

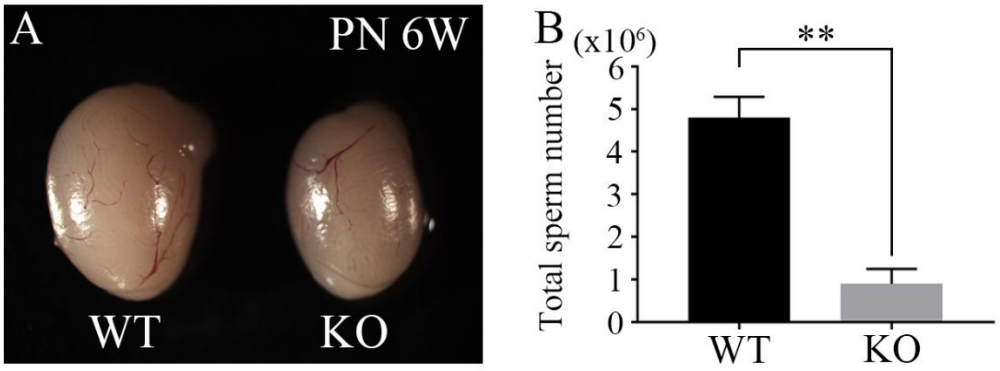

Figure 8. Analysis of testicular size and total sperm number between WT and *Mast4* KO mice

A) At PN 6W, the testes of *Mast4* KO mice are smaller than those of WT mice. B) The total sperm number in *Mast4* KO testes is significantly decreased (n = 4).

2.2. MAST4 expression pattern during spermatogenesis

The temporal and spatial expression pattern of MAST4 was examined in WT testes to identify the role of MAST4. At PN 1D, when developing germ cells were migrating in developing seminiferous tubules (Figure 9A), MAST4 was expressed in Sertoli cells expressing SRY-box transcription factor 9 (SOX9) and anti-Müllerian hormone (AMH) (Figure 9B, C arrowhead). At PN 3W, when testicular structures were fully developed (Figure 9D), the MAST4 expression shifted to Leydig cells being co-localized with 3β-hydroxysteroid dehydrogenase (3β-HSD) although SOX9 was continuously expressed in Sertoli cells (Figure 9E, F arrowhead). This result demonstrated that MAST4 expression shifted from Sertoli cells to Leydig cells at PN 3W.

Mast4 RNA localization was examined at PN 1D and PN 3W through *in situ* hybridization. At PN 1D, *Mast4* was expressed in Sertoli cells in the outermost layer of seminiferous tubules (Figure 10A, B). At PN 3W, *Mast4* was expressed in Leydig cells and spermatogonia (Figure 10C, D). The RNA expression pattern of *Mast4* partially supported its protein expression pattern mostly at testicular developmental stages.

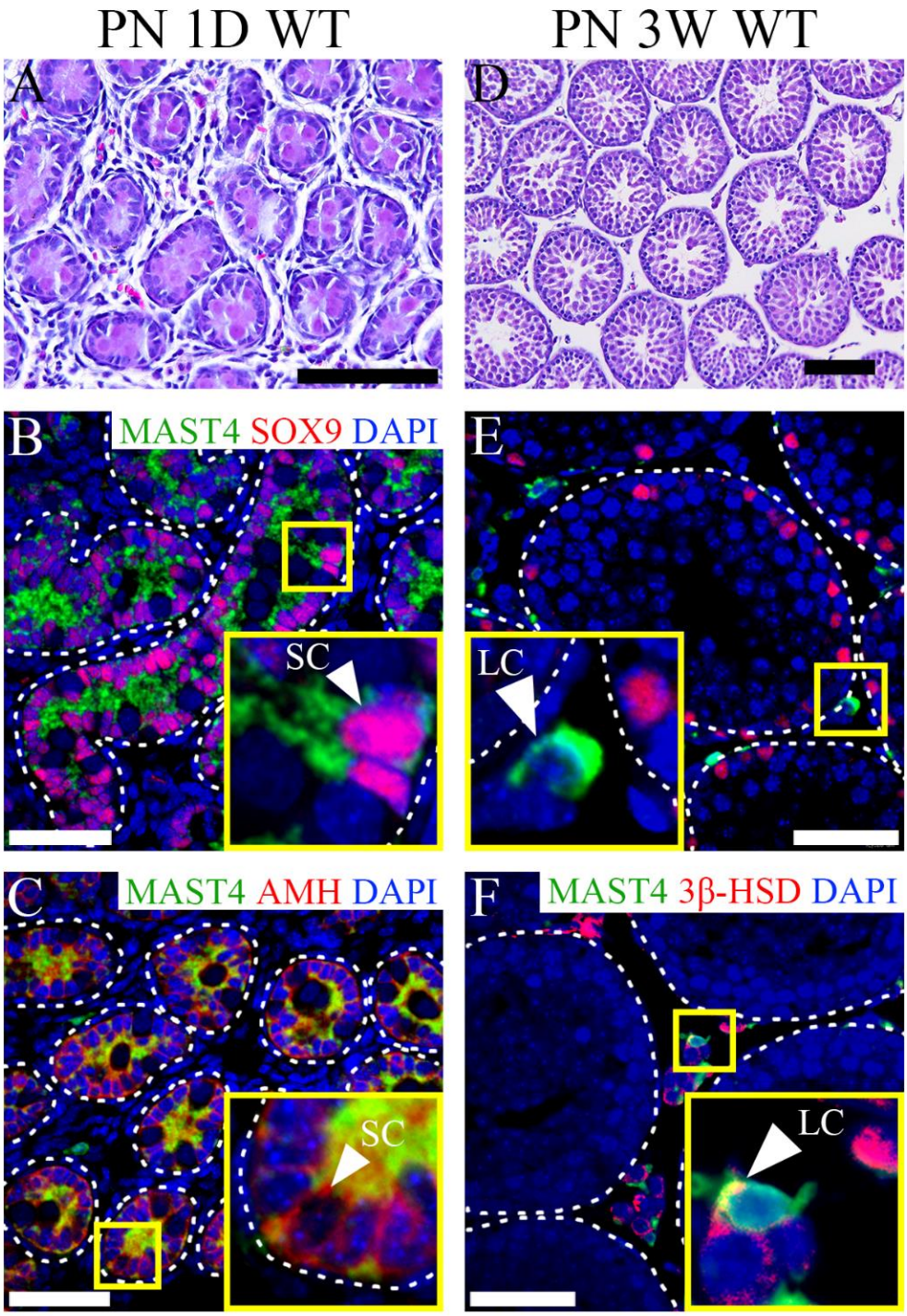

Figure 9. MAST4 expression pattern during testis development

A) At PN 1D, germ cells migrate in developing seminiferous tubules. B) MAST4 is expressed in the cytoplasm of the developing Sertoli cells, while SOX9 is expressed in their nuclei (arrowhead). C) Similarly, strong expression patterns of AMH are localized in the developing Sertoli cells with MAST4 co-localization (arrowhead). D) At PN 3W, the testes have a developed structure with differentiating spermatogonia and Leydig cells. E) The expression of MAST4 shifts to Leydig cells, while SOX9 is continuously expressed in Sertoli cells (arrowhead). F) MAST4 is expressed in Leydig cells with 3β-HSD co-localization (arrowhead).

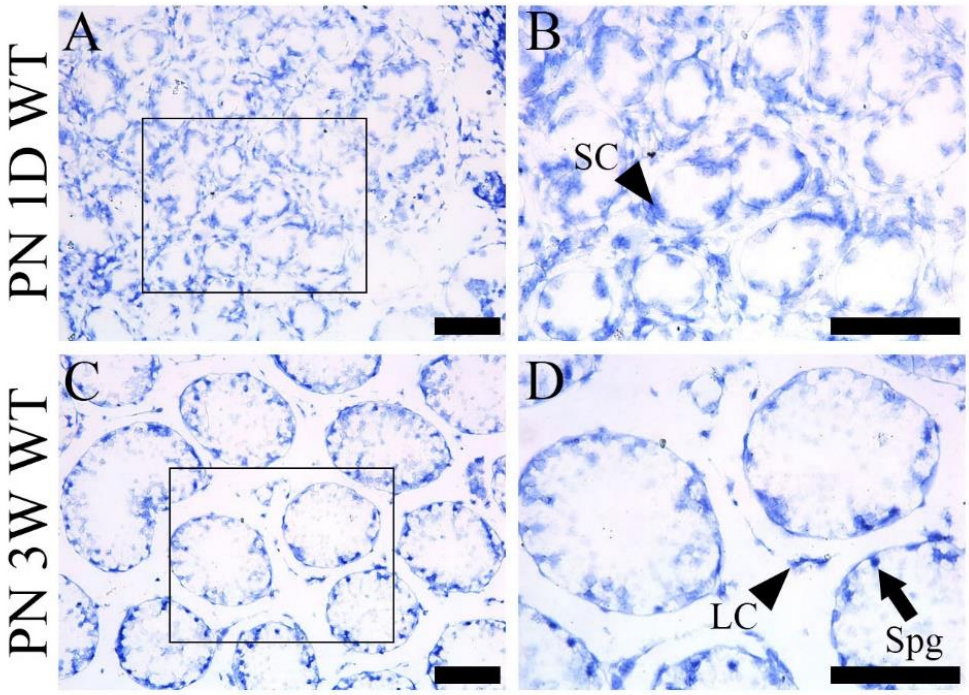

Figure 10. *In situ* hybridization of *Mast4* expression during testis development

Mast4 is examined in PN 1D and PN 3W testes through *in situ* hybridization. A) At PN 1D, *Mast4* is expressed in Sertoli cells. B) *Mast4* expression in Sertoli cells is in the outermost layer of seminiferous tubules (arrowhead). C) At PN 3W, *Mast4* is expressed in Leydig cells and spermatogonia. D) *Mast4* is strongly expressed in several spermatogonia (arrowhead; LC, arrow; Spg). Scale bars: 100 μm. SC: Sertoli cell; LC: Leydig cell; Spg: Spermatogonia.

2.3. Irregular seminiferous tubule structures in *Mast4* KO testes

Various testis markers were analyzed in PN 6W WT and *Mast4* KO mice to investigate the spermatogenic dysfunction in Mast4 KO testes. WT testes had compact seminiferous tubules with all types of germ cells (Figure 11A), while *Mast4* KO testes had several seminiferous tubules with depleted germ cells or Sertoli cells only, which is the characteristic SCO phenotype. In addition, the interstitial space was relatively wider and the seminiferous tubule lumen was enlarged because of degenerated germ cells in *Mast4* KO compared with those in WT testes (Figure 11B). Interestingly, the SCO phenotype in *Mast4* KO testes was observed in PN 21M WT testes (Figure 11C), indicating that *Mast4* KO and aged mouse testes shared a common point of the SCO phenotype.

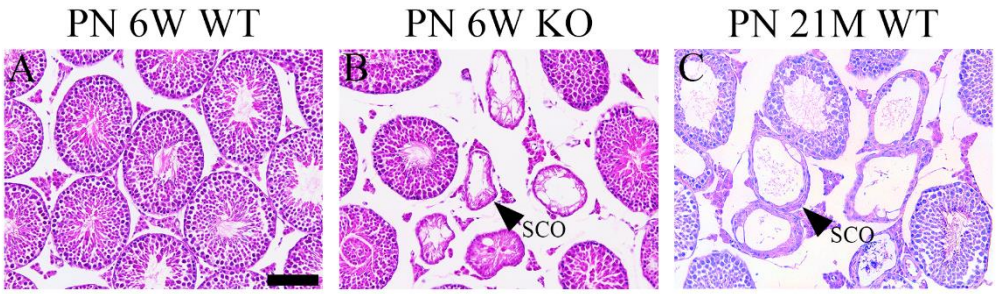

Figure 11. Sertoli cell-only tubular structure in *Mast4* KO and aged mouse testes

A) At PN 6W, the WT testes have compact seminiferous tubules with all types of germ cells. B) *Mast4* KO testes have seminiferous tubules with depleted germ cells or SCO morphology (arrowhead). C) PN 21M mice testes have SCO tubules similar to those in *Mast4* KO testes (arrowhead). SCO; Sertoli cell-only syndrome. Scale bars: 100 μm.

2.4. Sertoli cell-only tubule phenotype in *Mast4* KO testes

Various testis markers were analyzed in PN 6W WT and *Mast4* KO mice to investigate the spermatogenic dysfunction in *Mast4* KO testes. SOX9 was expressed in the nuclei of Sertoli cells in WT mice (Figure 12A). The number of SOX9-expressing Sertoli cells in the SCO tubules of *Mast4* KO mice increased (Figure 12B). DDX4, which was expressed in the spermatogonia of the WT testes (Figure 12C), was not observed in the SCO tubules although it was expressed in the normal seminiferous tubules in *Mast4* KO mice (Figure 12D). RNA-sequencing (RNA-seq) analysis showed that the expression of Sertoli cell markers, such as *Amhr2*, *Gata4*, *Sox9* and *Amh*, in the testes of *Mast4* KO mice increased (Figure 13A). Among the undifferentiated spermatogonium markers, *Id4* and *Gfra1* were not significant in *Mast4* KO mice compared with those in WT mice. *Bcl6b* and *Zbtb16* (also known as *Plzf*) in *Mast4* KO mice decreased (Figure 13B). Therefore, the development of seminiferous tubules as SCO morphology was disrupted with the increased expression of Sertoli cell markers in *Mast4* KO testes.

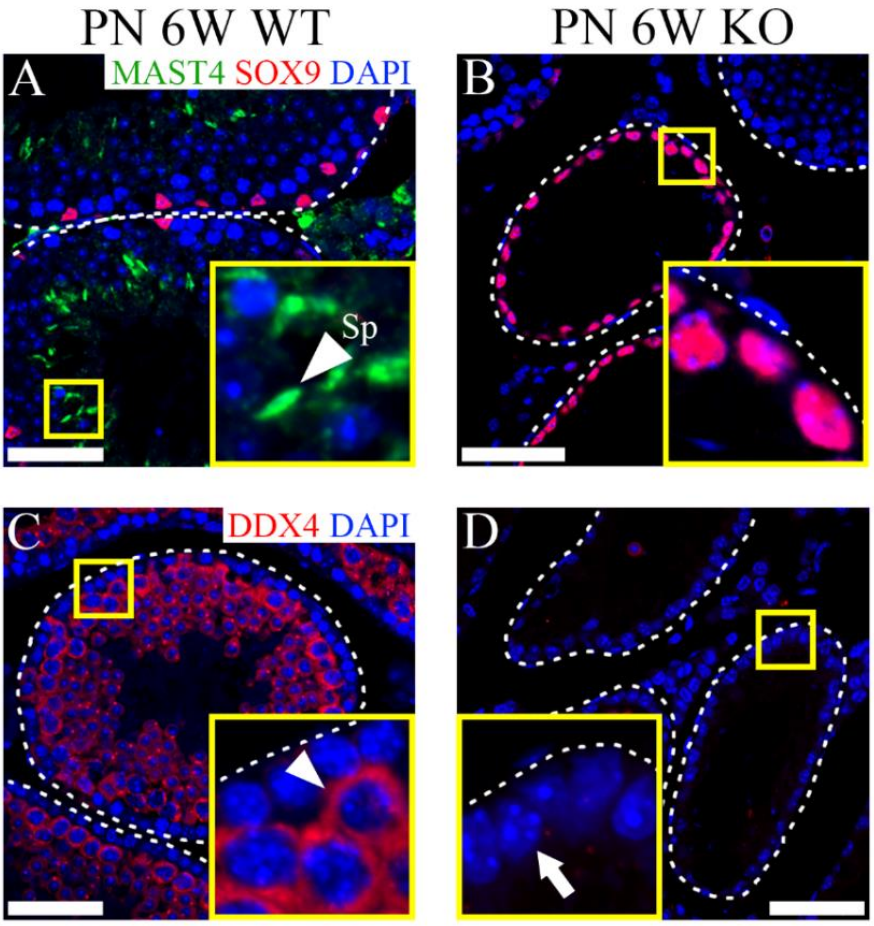

Figure 12. Comparison of testis marker expression between WT and *Mast4* KO testes

A) MAST4 is expressed in Leydig cells and spermatids although SOX9 is expressed in the nuclei of Sertoli cells in WT testes (arrowhead). B) In *Mast4* KO testes, SOX9 is strongly expressed in Sertoli cells not only in the outermost layer of SCO tubules but also in normal seminiferous tubules. C) DDX4 is expressed mainly in differentiating spermatogonia (arrowhead). D) In *Mast4* KO testes, DDX4 is not expressed in SCO tubules (arrow). Scale bars: 100 μm.

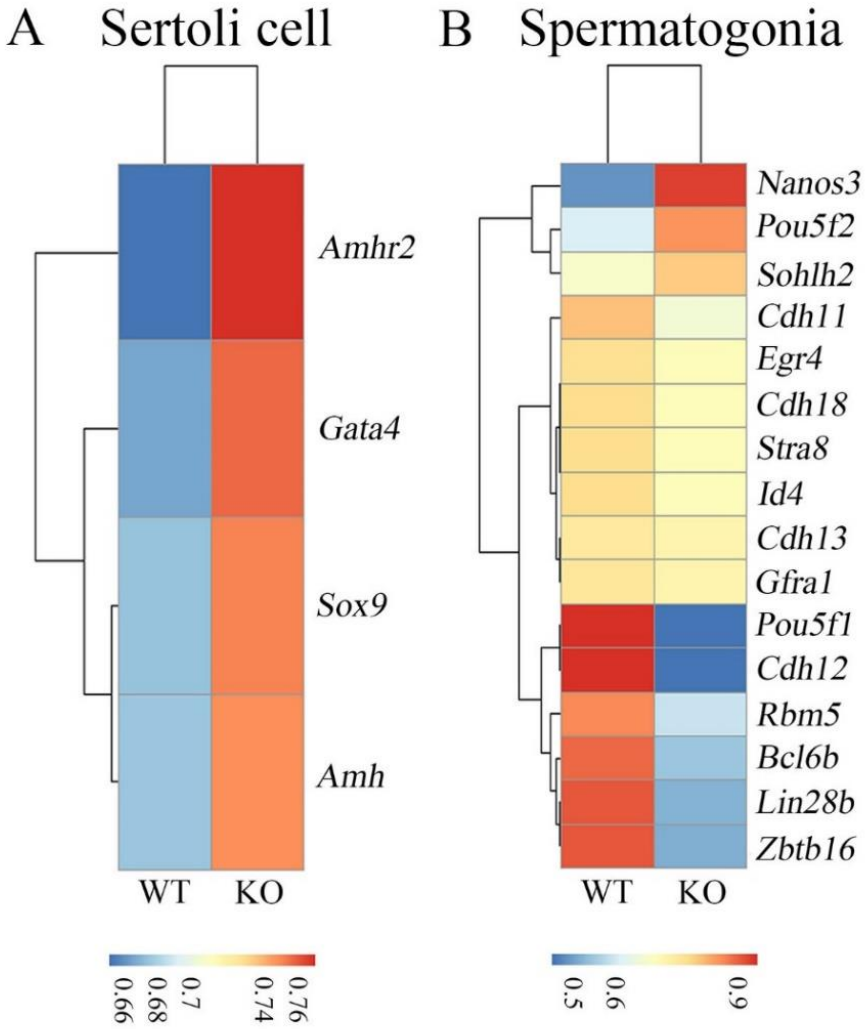

Figure 13. RNA-seq analysis in PN 6W WT and *Mast4* KO testes

A) In RNA-seq analysis, the expression of several Sertoli cell markers (*Amhr2*, *Gata4*, *Sox9*, *Amh*) in *Mast4* KO testes increased. B) The expression of spermatogonia differentially changed. *Nanos3* in *Mast4* KO testes significantly increased. The expression of *Id4* and *Gfra1* is not significant in *Mast4* KO testes compared with that in WT testes. *Bcl6b* and *Zbtb16* in *Mast4* KO testes decreased.

2.5. Differences in cell proliferation and apoptosis in *Mast4* KO testes

Proliferation and apoptosis were examined between PN 6W WT and *Mast4* KO testes. Proliferating cell nuclear antigen (PCNA) was expressed mostly in the outermost layer of the seminiferous tubules of WT mice (Figure 14A). However, PCNA was not expressed in the SCO tubules of *Mast4* KO mice although its expression remained similar to that in normal seminiferous tubules (Figure 14B). Terminal deoxynucleotidyl transferase dUTP nick end labeling (TUNEL) staining detected a few apoptotic cells in several spermatogonia of the seminiferous tubules of WT mice (Figure 14C) and a remarkable number of apoptotic cells in the outermost layer of the seminiferous tubules of *Mast4* KO mice (Figure 14D).

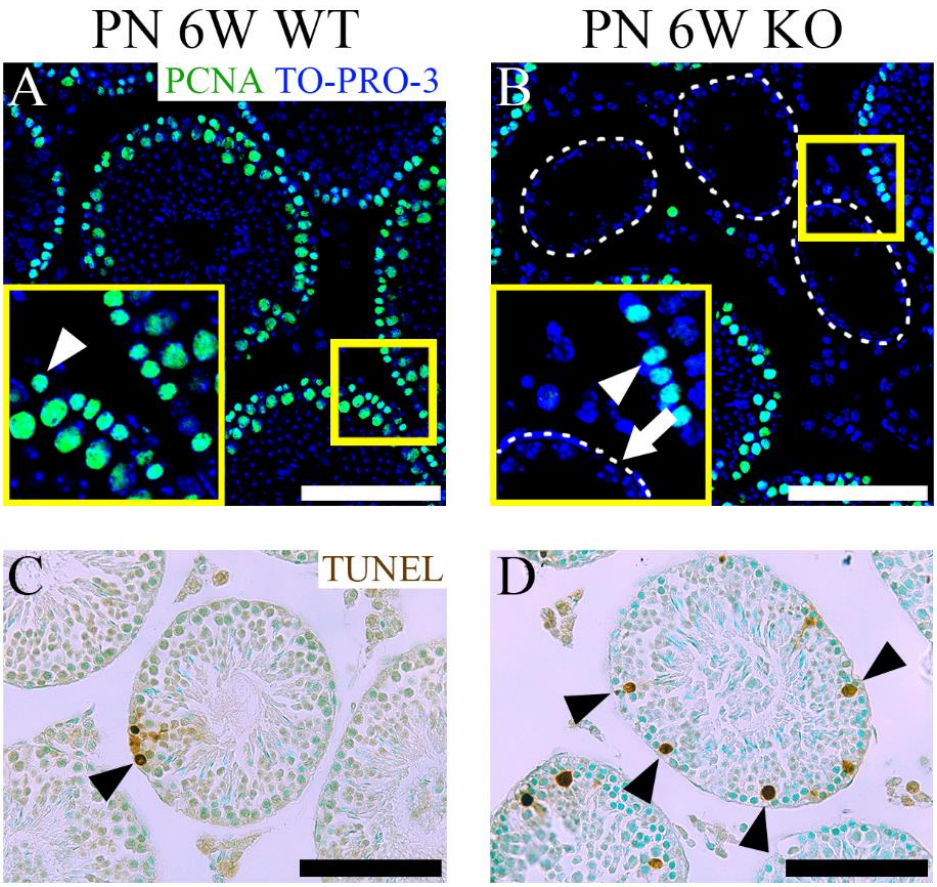

Figure 14. Proliferative and apoptotic marker expression between WT and *Mast4* KO testes

A) PCNA is expressed in the overall outermost layer of seminiferous tubules (arrowhead). B) In *Mast4* KO testes, PCNA is not expressed in SCO tubules (arrow) although its expression remained similar to normal seminiferous tubules (arrowhead). C) TUNEL staining detects a few apoptotic cells in spermatogonia in WT testes (arrowhead). D) In *Mast4* KO testes, apoptotic cells increased in the outermost layer of seminiferous tubules (arrowheads). Scale bars: 100 μm.

2.6. Effects of MAST4 on ERM transcription factor

Since the SCO phenotype in *Mast4* KO testes is similar to that in *Erm* KO testes, and FGF2 regulates SSC self-renewal through the ERM, the effects of FGF2 on the relationship between MAST4 and ERM was investigated in TM4 cells. In the presence of FGF2, the RNA expression of *Mast4* and *Erm* increased (Figure 15A). In addition, treatment with SU5402, which is an FGF receptor inhibitor, significantly decreased the expression of *Mast4* and *Erm* (Figure 15B, C). This result indicated that FGF2 regulated *Mast4* and *Erm* in Sertoli cells.

The ERM expression pattern was also examined in WT and *Mast4* KO mice at PN 6W to identify whether MAST4 affected ERM. ERM was expressed in Sertoli cells in WT mice and co-localized with SOX9-positive cells, along with several elongated spermatids (Figure 16A). Conversely, the ERM expression in *Mast4* KO mice decreased and was rarely observed even in SCO tubules (Figure 16B). The western blots of WT and *Mast4* KO TM4 cells showed that the ERM expression in the nucleus of *Mast4* KO cells decreased but did not change in the cytosol of the cells (Figure 16C). Therefore, the presence of FGF2 or the absence of MAST4 affected ERM expression.

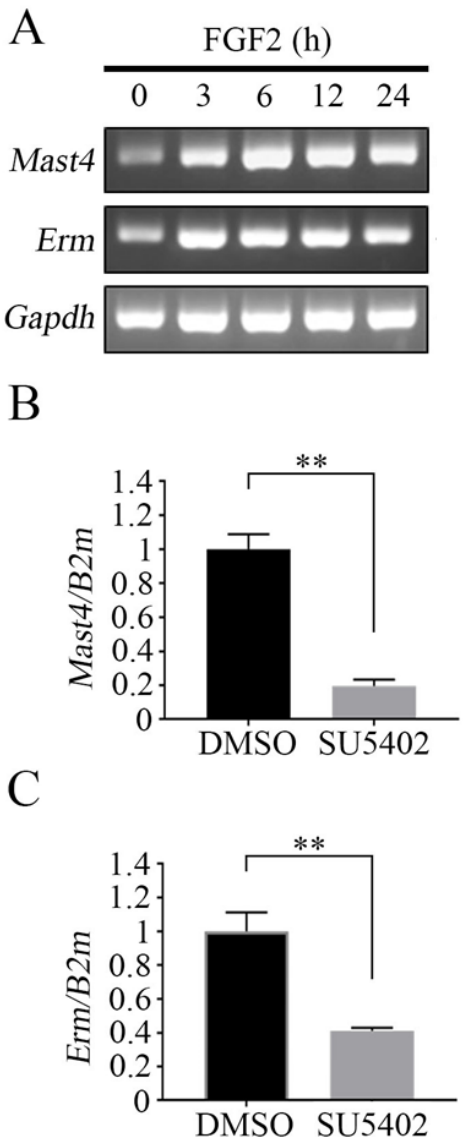

Figure 15. Effects of FGF2 on the expression of *Mast4* and *Erm*

A) In the presence of FGF2, the expression of *Mast4* and *Erm* in TM4 cells increased. B) After the effect of FGF signaling with SU5402 was inhibited, the *Mast4* expression significantly decreased (n = 3). C) Similar to the *Mast4* expression, the *Erm* expression decreased (n = 3).

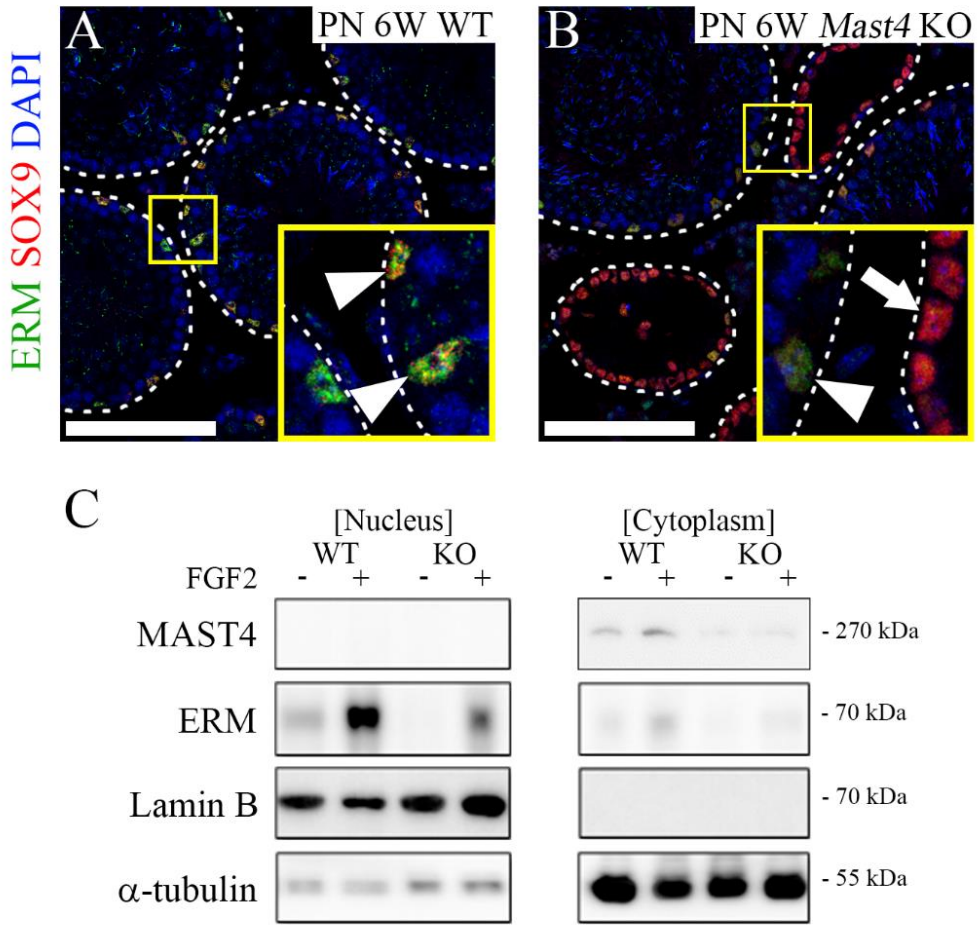

Figure 16. ERM expression in WT and *Mast4* KO

A) In PN 6W WT, ERM is expressed in Sertoli cells (arrowheads), along with several elongated spermatids. B) In PN 6W *Mast4* KO testes, the ERM expression pattern in normal seminiferous tubules (arrowhead) decreased and was rarely observed in the SCO tubules (arrow). C) TM4 cells were treated with FGF2 for 6 h. Nuclear/cytoplasmic fractions were analyzed by western blot. The basal and FGF2-induced ERM expression levels in MAST4-depleted TM4 cells decreased. Scale bars: 100 μm.

2.7. Regulation of genes related to SCC self-renewal via the MAST4–ERM interaction

To investigate the molecular relationship between MAST4 and ERM, we performed IP assay and observed the interaction between MAST4 and ERM (Figure 17A). Considering that MAST4 is a serine/threonine protein kinase and that ERM transactivation is regulated by phosphorylation, we further examined whether MAST4 induced ERM phosphorylation. Specifically, FGF2 increased p-serine of ERM, and MAST4 overexpression alone increased p-serine of ERM, whose level was similar to that induced by FGF2 (Figure 17B). Given that ERM is a transcription factor, we examined the ERM target genes through a luciferase assay. We found that the basal and FGF2-induced transcription levels of *Cxcl5* and *Cxcl12* were decreased by MAST4 depletion (Figure 18A, B). Conversely, MAST4 PDZ overexpression increased the transcription of *Cxcl5* and *Cxcl12* even in the absence of FGF2 stimulation (Figure 18C, D). In the same context, the RNA expression levels of *Erm*, *Cxcl5*, and *Cxcl12* in *Mast4* KO TM4 cells decreased (Figure 19A), but these levels significantly increased with MAST4 PDZ overexpression (Figure 19B).

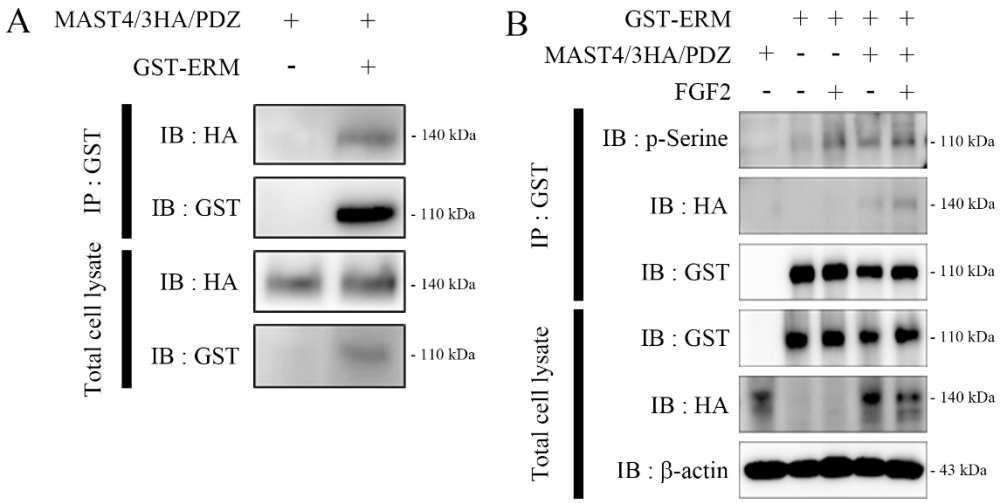

Figure 17. Interaction of MAST4 and ERM

A) Interaction between MAST4 and ERM was examined. GST-hERM and HA-hMAST4 PDZ were transiently co-transfected into TM4 cells and then subjected to GST pull-down. MAST4 interacted with ERM. B) GST-hERM and HA-hMAST4 PDZ were transiently co-transfected into TM4 cells and then treated with FGF2 for 6 h. GST-ERM was immunoprecipitated, and the complexes were analyzed by western blot. The bands, which were recognized by the p-serine antibody, were later reprobed with the GST antibody. ERM serine phosphorylation increased in the presence of MAST4.

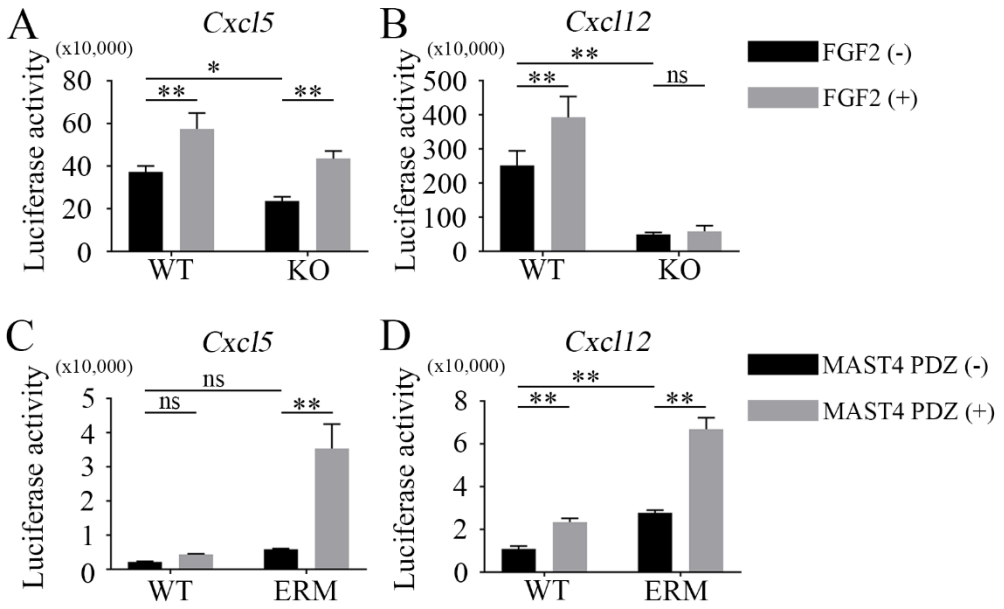

Figure 18. Transcriptional activities of ERM according to FGF2 and MAST4

A) *Cxcl5*- and B) *Cxcl12*-luciferase reporter and β-gal were co-transfected into the WT and MAST4-depleted TM4 cells. TM4 cells were then treated with 50 ng/ml of FGF2 for 18 h. The basal level and FGF2-induced increase in A) *Cxcl5* and B) *Cxcl12* transcription levels were decreased by *Mast4* depletion (n = 3). C) *Cxcl5*-luciferase reporter, D) *Cxcl12*-luciferase reporter, and β-gal were co-transfected with or without Flag-ERM and HA-hMAST4 PDZ into the WT TM4 cells for 24 h. The basal level and ERM-induced increase in C) *Cxcl5* and D) *Cxcl12* transcription levels were increased by MAST4 PDZ overexpression (n = 3). Luciferase assay was normalized with β-gal activity.

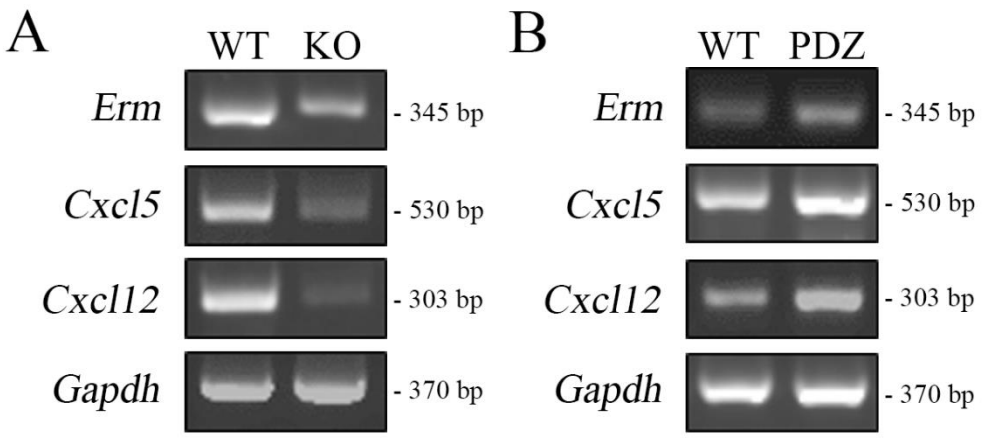

Figure 19. mRNA expression of *Erm* and ERM target genes according to MAST4

The mRNA expression of *Erm*, *Cxcl5*, and *Cxcl12* (A) decreased in MAST4-depleted TM4 cells, but (B) increased in TM4 cells transiently overexpressing HA-MAST4 PDZ.

2.8. MAST4-mediated phosphorylation of ERM at serine 367

We identified ERM serine sites that might be phosphorylated by MAST4 and involved in MAST4-induced ERM regulation and subsequent target gene expression. After mutating the well-known serine residues of ERM to alanine, we checked the mRNA expression level of ERM target genes, which were induced by the transient overexpression of ERM mutants in the presence of MAST4. Interestingly, ERM target genes were not induced when ERM serine 367 residue of ERM was substituted to alanine (ERM S367A; Figure 20A). To determine whether ERM serine 367 residue participated in MAST4-induced ERM phosphorylation, we performed and IP assay to examine the interaction between MAST4 and ERM or ERM S367A mutant and the level of ERM S367A mutant serine phosphorylation. The MAST4–ERM interaction and MAST4-induced ERM serine phosphorylation level were decreased by S367A mutation compared with those in ERM WT (Figure 20B).

On the basis of a previous study that reported how ERM S367A mutation decreased ERM-mediated transcription, we examined the transcription of ERM target genes induced by ERM WT or S367A mutant through a luciferase assay. ERM S367A mutation slightly decreased the basal level and MAST4-induced increase in *Cxcl5* and *Cxcl12* transcription compared with those in ERM WT

(Figure 21A, B). These results suggested that MAST4 interacted with ERM and induced serine 367 residue phosphorylation, eventually regulating ERM target genes related to SSC self-renewal.

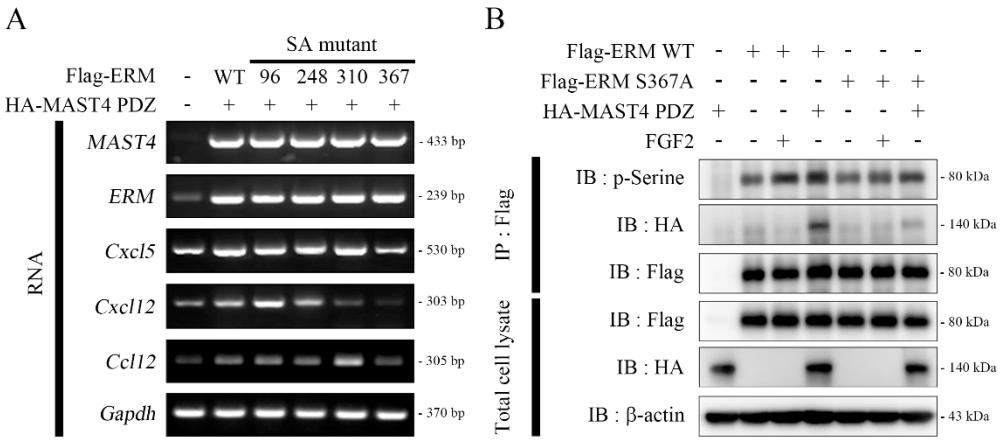

Figure 20. MAST4-mediated phosphorylation of ERM at serine 367

(A) The mRNA expression levels of *Mast4*, *Erm*, *Cxcl5*, *Cxcl12*, and *Ccl12* were examined using TM4 cells transfected with the WT and various phosphorylation inactive mutants of ERM in the presence of HA-hMAST4 PDZ for 24 h. ERM S367A mutant decreased the mRNA expression of *Cxcl5*, *Cxcl12*, and *Ccl12*. B) HA-hMAST4 PDZ, Flag-hERM WT, and Flag-hERM S367A were transiently co-transfected into TM4 cells, followed by FGF2 treatment for 6 h, as indicated. Flag-ERM was immunoprecipitated, and the complexes were analyzed by western blot. The bands, which were recognized by p-serine antibody, were later reprobed with the Flag antibody.

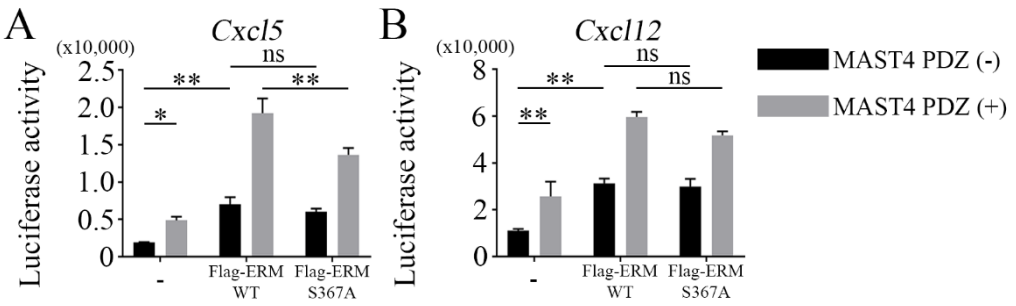

Figure 21. MAST4-mediated transcriptional activities of ERM at serine 367

A) *Cxcl5*- and B) *Cxcl12*-luciferase reporter and β-gal were co-transfected with Flag-ERM WT or Flag-ERM S367A into the WT TM4 cells in the absence or presence of HA-hMAST4 PDZ for 24 h. The basal level and MAST4-induced increase in *Cxcl5* and *Cxcl12* transcriptional activities were slightly decreased by the substitution of serine 367 of ERM by alanine (n = 3). A luciferase assay was normalized with the β-gal activity.

3. Discussion

MAST4 and its associated testis markers are harmoniously co-expressed, where the functional intensity is required during spermatogenesis. In this study, MAST4 was stage-dependently localized in seminiferous epithelia and Leydig cells. From the early developmental stage, MAST4 was localized in Sertoli cells and co-expressed with SOX9 and AMH. SOX9 plays a crucial role in testis development and adult testis maintenance (Lavery et al., 2011, Rahmoun et al., 2017). AMH is one of the first genes to be switched on in Sertoli cells during fetal development in mice and humans; it is also expressed continuously as long as Sertoli cells are immature (Rey & Grinspon, 2011, Sharpe et al., 2003). After PN 3W, the MAST4 expression shifts to spermatids and Leydig cells, which produce testosterone. Overall, MAST4 controls the functional activities of Sertoli cells before the puberty stage, which regulates SSC self-renewal acting as a pivotal role in the stem cell niche. After puberty, MAST4 regulates testis maturation, indicating that MAST4 plays an indispensable role in securing spermatogenesis.

MAST4 participates in the FGF2 signaling pathway. FGFs induce many kinases, including mitogen-activated protein kinase/extracellular signal-regulated kinase (MAPK/ERK) and phosphatidylinositol 3-kinase/protein

kinase B (PI3K/AKT); they also activate their signaling pathways (Park et al., 2010). Currently, FGF2 treatment increases the *Mast4* and *Erm* expression, while FGF2 inhibition decreases their expression level. MAST4 binds to ERM and positively regulates its transcriptional activity during the induction of the target genes related to SSC self-renewal. However, ERM expression in all SCO tubules of Mast4 KO testes significantly decreased, suggesting that SSC self-renewal was inhibited. In addition, the transcription and mRNA expression of ERM target genes (*Cxcl5* and *Cxcl12*) are downregulated in *Mast4* KO cells. Studies have also reported that FGF2 activates ERM expression (Ishii et al., 2012), and our results showed that FGF2 might induce ERM through MAST4 to promote SSC self-renewal.

IV. Section II : MAST4 controls cell cycle in SSCs

1. Introduction

SSCs undergo self-renewal strictly controlled by Sertoli cells through the secretion of specific factors such as GDNF and ERM (Chen & Liu, 2015). PLZF protein belongs to the Krüppel-like zinc finger protein family, which regulates diverse cellular processes, including cell proliferation, apoptosis, differentiation, and development (Pearson et al., 2008). PLZF controls the expression of cell cycle-related genes such as *p21*, *p53* (Choi et al., 2014), *Ccna2* (Costoya et al., 2008), and *c-Myc* (McConnell et al., 2003), thereby instructing stem/progenitor cells to accept certain cell fate programs for self-renewal or differentiation. Therefore, the cell cycle mechanism of SSCs by PLZF should be further explored in detail.

In marking cells involved in DNA synthesis, radioactive thymidine was replaced by halogenated nucleotides (e.g., IdU, BrdU, and CldU), which can be recognized by specific antibodies after they are incorporated into newly synthesized DNA (Hughes et al., 1958). Thymidine analogs are taken up by cells during the S phase and act as proxy markers of cells in this phase of the cell cycle. Through the analysis of a population of cells progressing through the S

phase, the mean S phase duration (T_s) and total cell cycle duration (T_c) can be calculated (Harris et al., 2018). Measuring T_s and T_c within SSC populations can provide important insights into MAST4 that regulates the cell cycle of SSCs.

In this section, a tissue culture system was introduced to control the cell cycle of the mouse testis. Because the testis is composed of various cell populations, culturing with only one type of cell to prove the mechanism is inappropriate. Therefore, it provides knowledge about the mechanism of controlling the cell cycle by using the upstream and downstream molecules that regulate MAST4.

2. Results

2.1. MAST4-induced regulation of SSC self-renewal

The mechanisms by which *Mast4* KO leads to SSC self-renewal were examined to determine the changes in SSCs in the seminiferous tubules of WT and *Mast4* KO testes. In PN 6W WT testes, PLZF was localized sparsely in the outermost layer of seminiferous tubules (Figure 22A), whereas its expression in *Mast4* KO testes decreased (Figure 22B). The PLZF expression increased in PN 22W testes increased compared with that in PN 6W testes (Figure 22C); conversely, its expression in *Mast4* KO testes decreased compared with that in the WT (Figure 22D). The quantification analysis of immunohistochemistry indicated that PN 6W mice did not significantly differ between WT and KO testes (Figure 22E). In addition, the western blot analysis of PN 6W and PN 22W testes revealed that the PLZF expression in PN 22W *Mast4* KO testes significantly decreased (Figure 22F). Thus, *Mast4* deletion led to depleted germ cells and SCO tubules in the testes and significantly decreased the PLZF expression in the adult stage.

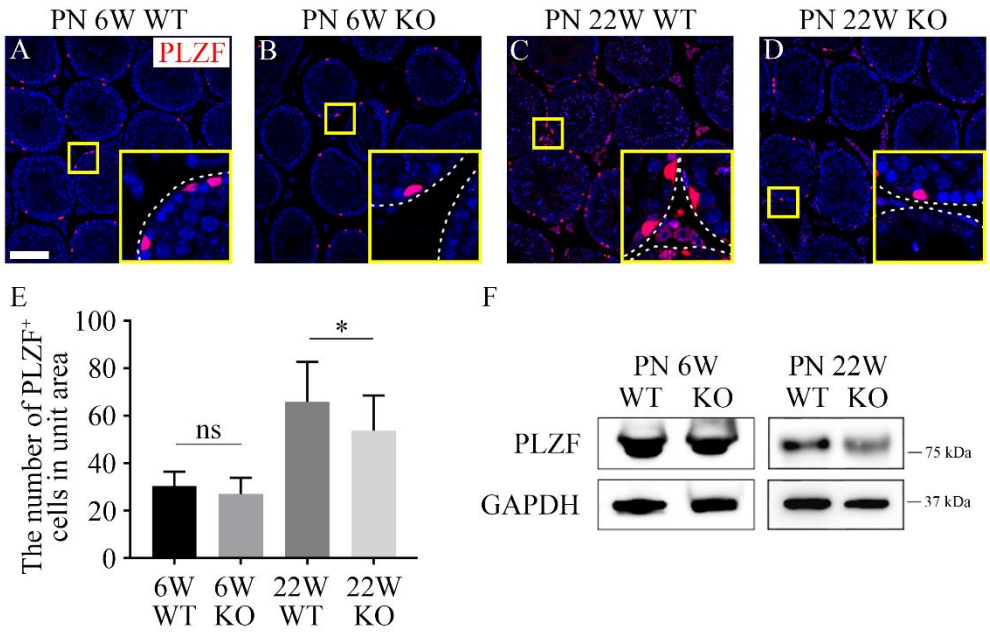

Figure 22. PLZF expression between WT and *Mast4* KO testes

(A–D) Immunohistochemistry of PLZF in WT and *Mast4* KO testes. PLZF is localized in spermatogonial stem cells in the outermost layer of seminiferous tubules. In comparison with the PLZF expression in (A) PN 6W and (C) PN 22W WT testes, the PLZF expression in (B) PN 6W and (D) PN 22W KO testes decreased. (E) Quantification of the PLZF expression in WT and *Mast4* KO testes (n = 15, five images per group of three mice). (F) Western blot of WT and *Mast4* KO testes in PN 6W and PN 22W mice. (E, F) PLZF expression significantly decreased in PN 22W KO mice but not in PN 6W KO mice. Scale bars: 100 μm.

2.2. Cell cycle alteration of SSCs in *Mast4* KO testes

Since the self-renewal of SSCs was not properly regulated in *Mast4* KO testes, their cell cycle was examined to understand the cellular mechanisms involved. Cell cycle time (T_c) was calculated by 5′-iodo-2′-deoxyuridine (IdU)/5′-bromo-2′-deoxyuridine (BrdU) injection at 12 h intervals between WT and *Mast4* KO testes. PLZF was also examined to label SSCs, and the co-localization of IdU-only-labeled cells and PLZF-labeled cells was checked in serial sections. The SSCs in each group had average T_c of 87.8, 94.8, 58.4, and 124 h, respectively (Figure 23A-H). T_c was not significantly different between PN 6W WT and *Mast4* KO SSCs (Figure 23I), but it was significantly increased in PN 22W *Mast4* KO compared with that in the corresponding WT SSCs (Figure 23J). Therefore, T_c of SSCs increased not in pubertal stages but in adult stages of *Mast4* KO mice, indicating that the cell cycle decreased in adult *Mast4* KO SSCs.

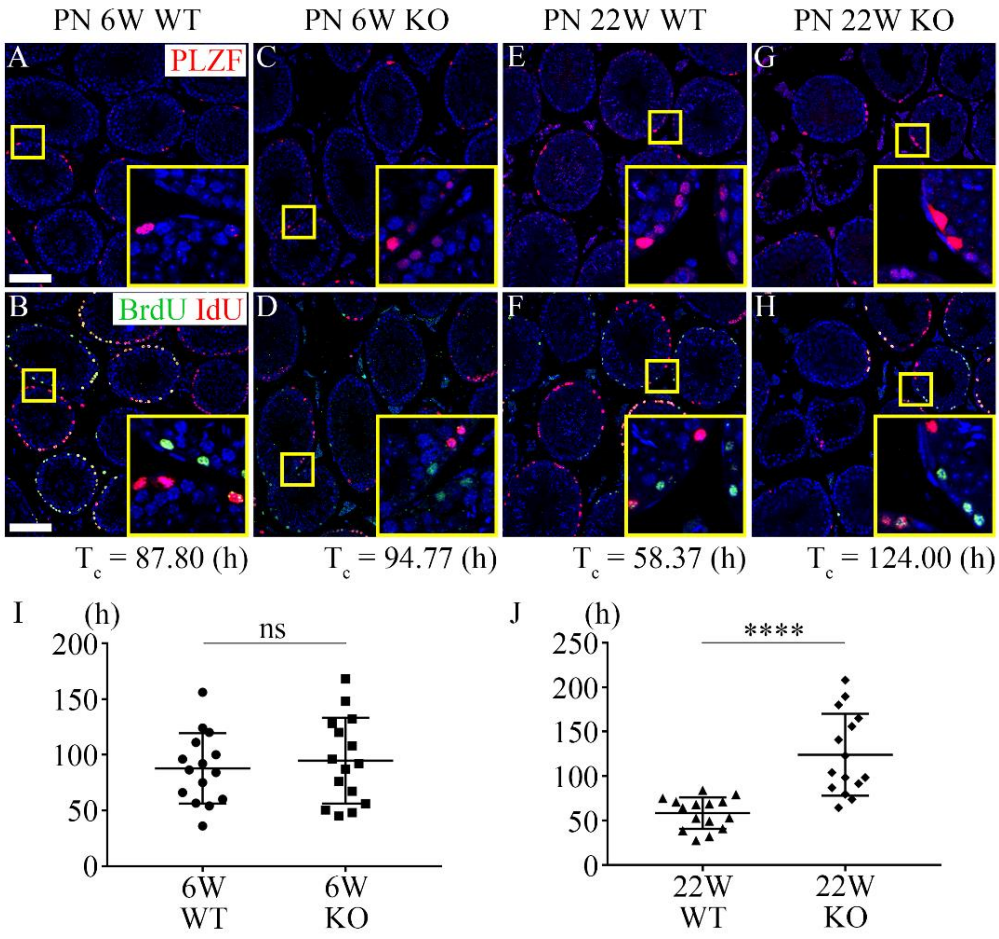

Figure 23. Cell cycle analysis between WT and *Mast4* KO spermatogonial stem cells

(A–H) Immunohistochemistry of IdU/BrdU and PLZF for the cell cycle calculation of SSCs in WT and *Mast4* KO testes. Cell cycle time is calculated from the co-localization of IdU-only-labeled and PLZF-labeled cells by serial sectioning. (I) Cell cycle time in PN 6W KO SSCs is similar to that in WT SSCs. (J) The cell cycle time in PN 22W KO SSCs is dramatically increased compared with that in WT SSCs (n = 15). Scale bars: 100 μm.

2.3. Effects of MAST4 on the mechanism involved in the cell cycle of SSCs

The molecular mechanism of MAST4 was investigated to determine how it regulates the cell cycle of SSCs. CDK2 is a key regulator of the G1–S transition in stem cells by phosphorylating PLZF. An IP assay confirmed the interaction between PLZF and CDK2 (Figure 24A). The expression of CDK2 and PLZF target genes was examined in PN 22W WT and *Mast4* KO testes to determine whether *Mast4* deletion affects CDK2-PLZF mechanisms in SSCs. While CDK2 was observed in the outermost layer of seminiferous tubules in WT testes (Figure 24B), MAST4 depletion reduced the CDK2 expression (Figure 24C). Western blotting of PN 22W WT and *Mast4* KO testes also showed that the expression of CDK2 in *Mast4* KO testes decreased (Figure 24D). In *Mast4* KO testes, the p21 expression significantly increased, and the p53 expression slightly increased (Figure 25A-D). The western blot and RT-qPCR analysis showed similar results (Figure 25E-G). Therefore, CDK2 directly interacts with PLZF, and MAST4 regulates the expression of CDK2 and PLZF; subsequently, the expression level of PLZF target genes.

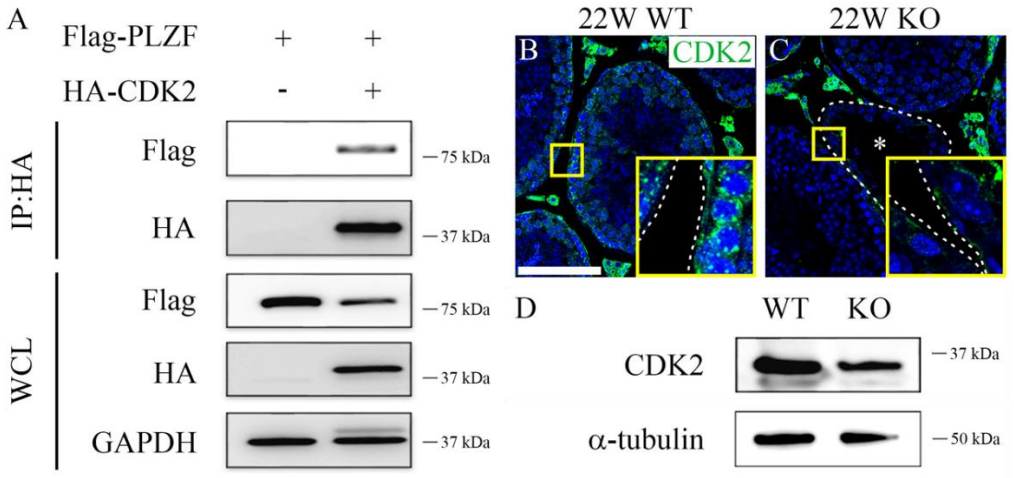

Figure 24. PLZF–CDK2 interaction and MAST4-mediated CDK2 expression

(A) Interaction between PLZF and CDK2 is examined. Flag-PLZF and HA-CDK2 were transiently co-transfected into HEK293T cells, followed by HA pull-down. PLZF interacts with CDK2. (B) In PN 22W WT testes, CDK2 is expressed in the cytoplasm of spermatogonia in the outermost layer of seminiferous tubules. (C) CDK2 expression is significantly decreased in PN 22W *Mast4* KO testes compared with that in WT testes. Asterisks indicate SCO tubules. (D) Western blot analysis of PN 22W WT and *Mast4* KO testes indicates that CDK2 expression is decreased in PN 22W *Mast4* KO testes. Scale bars: 100 μm.

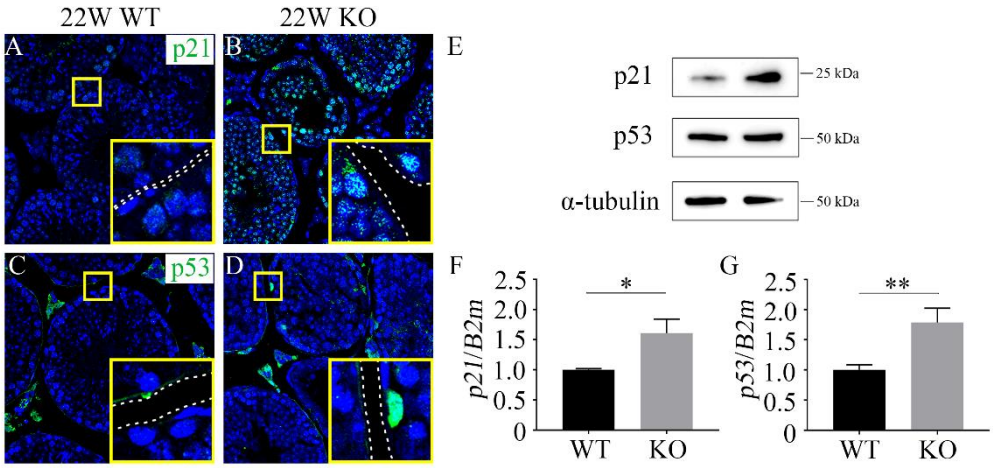

Figure 25. Cell cycle-related gene expression between WT and *Mast4* KO testes

(A) In PN 22W WT testes, p21 is rarely expressed in seminiferous tubules. (B) p21 expression is significantly increased in PN 22W *Mast4* KO testes compared with that in the WT. (C) In PN 22W WT testes, p53 is rarely expressed in seminiferous tubules. (D) p53 expression is slightly increased in PN 22W *Mast4* KO testes compared with that in the WT. (E) Western blot analysis of PN 22W WT and *Mast4* KO testes indicates that the p21 expression in PN 22W *Mast4* KO testes is increased, and p53 levels are not significantly changed. (F, G) RT-qPCR analysis indicates that the mRNA expression levels of (F) *p21* and (G) *p53* in PN 22W *Mast4* KO testes are significantly increased compared with those in WT testes. Scale bars: 100 μm.

2.4. Increased interaction of PLZF and CDK2 by CXCL12

An immunoprecipitation assay between PLZF and CDK2 was performed after CXCL12 treatment to investigate whether the interaction of PLZF and CDK2 could be affected by MAST4. As a downstream of MAST4, CXCL12 increased the interaction of PLZF and CDK2 (Figure 26), indicating that the FGF2/MAST4/CXCL12 pathway from Sertoli cells could regulate the function of PLZF and CDK2 in SSCs.

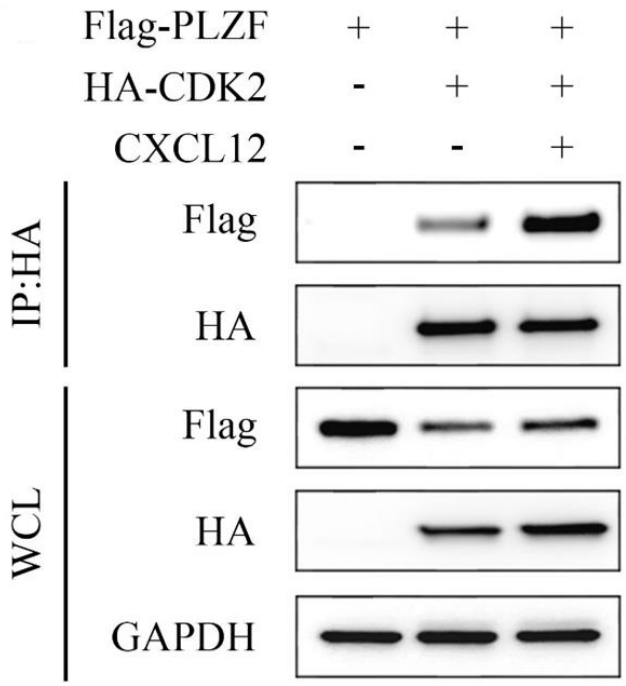

Figure 26. Effect of CXCL12 on the interaction between PLZF and CDK2

The effect of CXCL12 on the interaction between PLZF and CDK2 is examined. Flag-PLZF and HA-CDK2 were transiently co-transfected into HEK293T cells and then treated with CXCL12 (100 ng/ml) for 24 h. CXCL12 increased the interaction between PLZF and CDK2.

2.5. FGF2/MAST4/CXCL12 pathway on the seminiferous tubular structure

An *in vitro* tissue culture of PN 1D WT and *Mast4* KO testes was utilized to determine whether the reduced cell cycle of SSCs could be rescued by the FGF2/MAST4/CXCL12 pathway. Exogenous FGF2 and CXCL12 were added to the culture medium to induce the MAST4 pathway. After 1 week of culturing, WT testes had well-organized seminiferous tubular structures, as revealed by HE staining (Figure 27A). However, *Mast4* KO testes had an irregular spermatogonium structure and a wider interstitial space than WT testes (Figure 27B). Exogenous FGF2 and CXCL12 rescued the enlarged interstitial space in *Mast4* KO testes similar to the WT (Figure 27C). Quantification analysis indicated that the interstitial space of the KO testes was significantly increased compared with that of the WT, and KO testes cultured with FGF2 and CXCL12 (KO+F+C) showed a decreased interstitial space area compared with that of the KO testes (Figure 27D). The expression of SSC proteins was then examined using immunohistochemistry. The PLZF expression decreased to the extent that it was invisible in *Mast4* KO testes and recovered in KO+F+C testes, similar to the WT (Figure 28A-C).

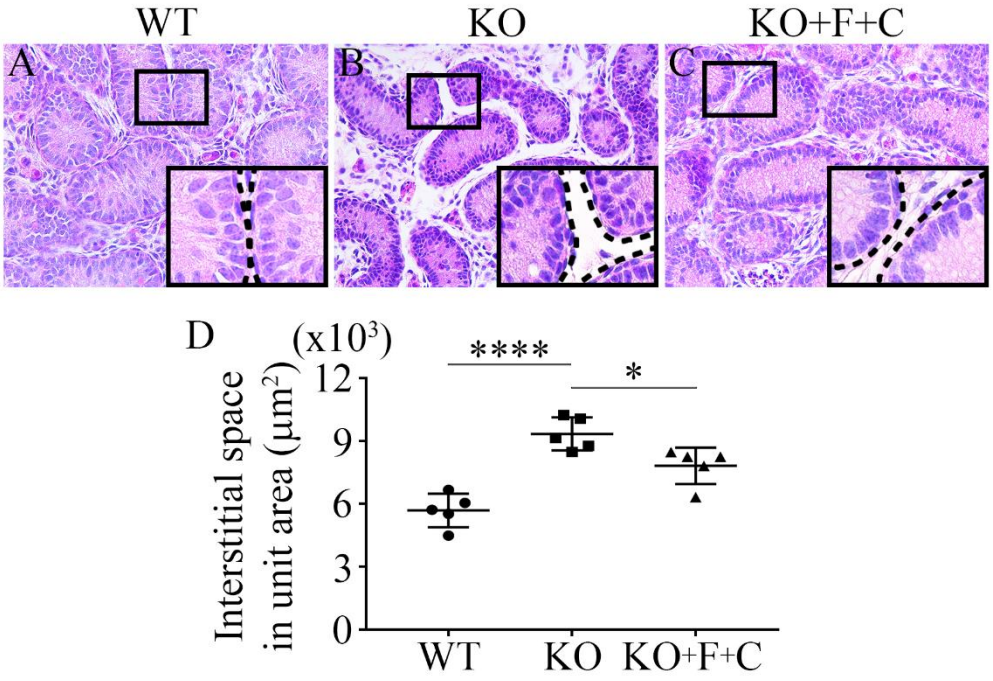

Figure 27. Testicular structure of *Mast4* KO testes according to FGF2 and CXCL12

(A) WT testes have well-organized seminiferous tubules. (B) *Mast4* KO testes have an irregular tubular structure and a wider interstitial space than the WT. (C) The structure of seminiferous tubules of KO+F+C testes is similar to that of the WT. (D) Quantitative analysis of the interstitial space in culture testis tissue. KO testes had a significantly widened area compared with the WT. KO+F+C testes have a decreased interstitial space. Scale bars: 100 μm.

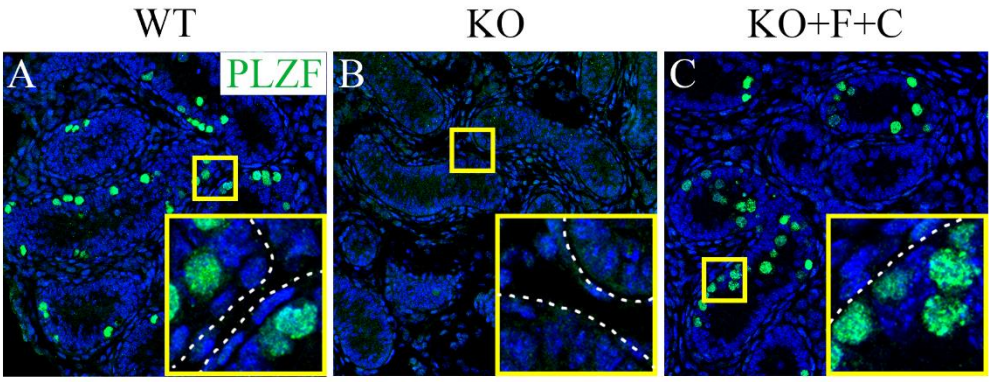

Figure 28. PLZF expression according to FGF2/MAST4/CXCL12

Immunohistochemistry analyses of PN 1D testes cultured for 1 week. (A) In WT testes, PLZF is sparsely localized in the outermost layer of seminiferous tubules. (B) PLZF expression is not observed in KO testes. (C) PLZF expression in KO+F+C testes is similar to that in WT. Scale bars: 100 μm.

2.6. FGF2/MAST4/CXCL12 pathway on the cell cycle of SSCs

The expression levels of the PLZF target genes p21 and p53 were examined. Their expression was rarely observed in the spermatogonia; however, their expression was significantly increased in KO testes and recovered in KO+F+C testes (Figure 29A-F). These results were also supported by RT-qPCR analyses. The expression levels of *p21* and *Ccna2* increased in *Mast4* KO mice and recovered in the KO+F+C testes (Figure 29G, H). Although *p53* expression was not significantly changed in KO testes, it was decreased in KO+F+C testes compared with that in the other groups (Figure 29I). Therefore, the FGF2/MAST4/CXCL12 pathway is crucial for maintaining the cell cycle of SSCs by regulating PLZF and its target gene expression.

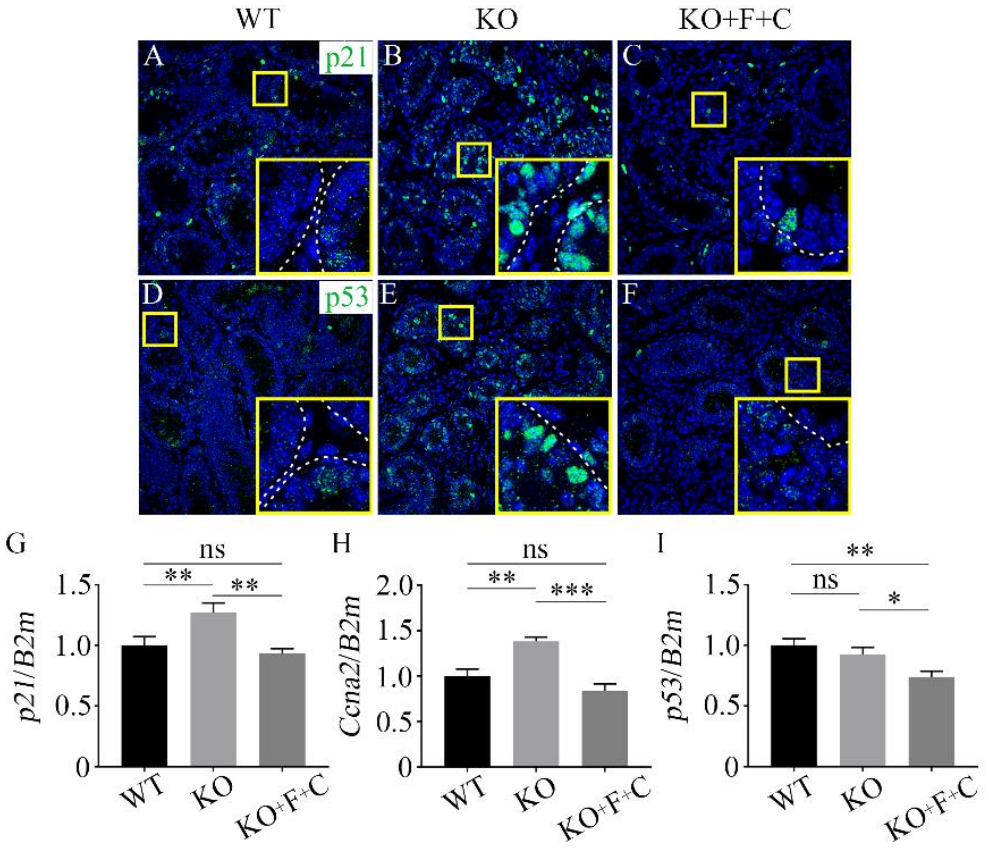

Figure 29. Cell cycle rescue of *Mast4* KO testes according to FGF2 and CXCL12

(A) p21 is expressed sparsely in the seminiferous tubules in WT testes. (B) p21 expression is dramatically increased in KO testes. (C) The p21 expression in KO+F+C testes is similar to that in WT. (D) p53 is rarely expressed in seminiferous tubules of WT testes. I p53 expression is significantly increased in KO testes. (F) In KO+F+C testes, p53 expression is similar to that in WT. (G) *p21* and (H) *Ccna2* expression is increased in KO testes and decreased in KO+F+C testes similar to that in the WT. (I) While *p53* expression is comparable between WT and KO testes, it is significantly decreased in KO+F+C testes compared with that in the other groups. Scale bars: 100 μm.

3. Discussion

MAST4 harmoniously exerted its functions by regulating various properties during spermatogenesis in a stage-dependent manner. In the pubertal stage (PN 6W), the testis size and sperm count of KO mice decreased compared with those of WT mice; however, the PLZF level did not significantly reduce. Notably, the PLZF expression significantly decreased in adult (PN 22W) KO testes compared with that in WT testes. Therefore, the failure of SSC self-renewal caused by *Mast4* deletion just began or did not proceed significantly in the pubertal stage.

CDK2, which regulates cell cycle, especially the G1 phase, interacts with PLZF and suppresses the transcription of *Ccna2* (Costoya et al., 2008, Yeyati et al., 1999). Although PLZF has been extensively studied as a marker of SSCs in various animal models (Costoya et al., 2004, Fayomi & Orwig, 2018, Sharma et al., 2019, Song et al., 2020), CDK2 has been rarely investigated in SSCs (Singh et al., 2019), and its role has been studied mostly in meiosis (Chauhan et al., 2016, Satyanarayana et al., 2008, Viera et al., 2015). The regulation of the interaction between PLZF and CDK2 is difficult to accurately investigate because MAST4 is expressed and involved in Sertoli cells, and it only transmits a signal to SSCs. To overcome this problem, we examined the expression of

CDK2 and PLZF in *Mast4* KO testes and the effect of CXCL12 on the interaction between CDK2 and PLZF. Because CXCL12 becomes activated and then transmits the paracrine signal from Sertoli cells to SSCs via the FGF2-MAST4-ERM pathway. CDK2 expression decreased in adult *Mast4* KO testes, whereas the interaction between CDK2 and PLZF increased after CXCL12 treatment.

A tissue culture system was introduced to regulate the mechanisms of various cell populations in the testis that cannot be resolved in cell culture. The *in vitro* tissue culture of the testes revealed irregular tubular structures and widened interstitial spaces in *Mast4* KO mice, which were recovered by FGF2 and CXCL12. In addition, the expression of SSC-related proteins, such as PLZF and c-Kit, was downregulated in *Mast4* KO testes. As such, we examined whether the reduced cell cycle progression could be restored through the MAST4 pathway. The function of PLZF in KO + F + C testes was similar to that in WT testes, as shown by immunohistochemistry and RT-qPCR analysis of PLZF target genes. Therefore, the cell cycle of SSC was regulated within the signaling pathway in which MAST4 operates.

V. GENERAL DISCUSSION

Mammalian spermatogenesis is a classic adult stem cell-based process regulated by mitosis and meiosis and supported by the self-renewal and differentiation of SSCs. Studies on SSCs have provided a model to better understand adult stem cell biology, and understanding the mechanisms that control SSC functions may lead to the treatment of male infertility. SSC self-renewal during spermatogenesis is a necessary process for transferring gametes to the next generation, and the cell cycle of SSCs should be well maintained during this process. The present study suggests that MAST4 is involved in maintaining the cell cycle of SSCs and regulating their self-renewal ability.

Mast4 KO testes undergo germ cell depletion and finally attain the SCO morphology. PLZF is critical for maintaining SSCs in a low proliferative state and regulating their cell cycle status (Sharma et al., 2019). On the basis of the decreased expression of PLZF and c-Kit in the present study, we suggested that MAST4 depletion lowered the self-maintenance capacity of SSCs and blocked spermatogonial differentiation. In humans and monkeys suffering from SCO syndrome, undifferentiated spermatogonia markers are decreased in a pattern similar to the RNA-seq analysis results of this study (Lau et al., 2020, Paduch et al., 2019b). In addition, the total sperm number significantly decreased in *Mast4*

KO mice, indicating that *Mast4* KO mice also exhibited spermatogenic dysfunction. Although the SCO tubules without germ cells are markedly atrophied, several normal seminiferous tubules show active spermatogenesis and produce sperms because of the expression of several genes, including DDX4 and PCNA. On the basis of these results, we could conclude that MAST4 was closely associated with spermatogenesis and could regulate the functions of Sertoli cells in SSC self-renewal, Leydig cells in testosterone production, and spermatids that give rise to sperms. In addition, we should verify the relationship between *Mast4* KO and aging, such as similar results between *Mast4* KO mice and aged mice, depleted germ cells, and SCO morphology.

Erm KO and *Plzf* KO mice exhibited agametic seminiferous tubules similar to those in *Mast4* KO mice (Chen et al., 2005, Sharma et al., 2019). As *Mast4* KO testes shared the same morphology with *Erm* KO and *Plzf* KO testes, mechanisms that regulate SSC self-renewal likely have common features. In the present study, the expression of ERM target genes involved in SSC self-renewal and SSC cell cycle via PLZF significantly decreased in *Mast4* KO testes. This finding suggested that the role of MAST4 in the previously discovered self-renewal mechanism through Sertoli cell–SSC interaction and its regulation via the cell cycle were newly revealed.

VI. CONCLUSION

This study showed that MAST4 is tightly related to spermatogenesis. FGF signaling plays a major role in regulating SSC self-renewal during spermatogenesis. The ERM transcription factor mediates the FGF2 signaling pathway. MAST4 phosphorylates ERM and regulates its transcriptional activity. The transcription of ERM target genes (*Cxcl5* and *Cxcl12*) coordinates SSC self-renewal. CXCL12 migrates to SSCs and transmits signals involved in SSC self-renewal. CDK2 phosphorylates PLZF that subsequently suppresses the transcription of *p21*, *p53*, and *Ccna2*. When the transcription of PLZF target genes is inhibited, SSCs can maintain their cell cycle. This study provided new insights into a novel mechanism by which MAST4 regulates ERM and PLZF involved in SSC self-renewal. Moreover, our findings not only suggested the significance of apprehending spermatogenesis but also reflected its potential therapeutic use for spermatogenic dysregulation. In summary, this study suggested that MAST4 not only has the potential for preventing male infertility but also has a role in stem cell maintenance in other organs (Figure 30).

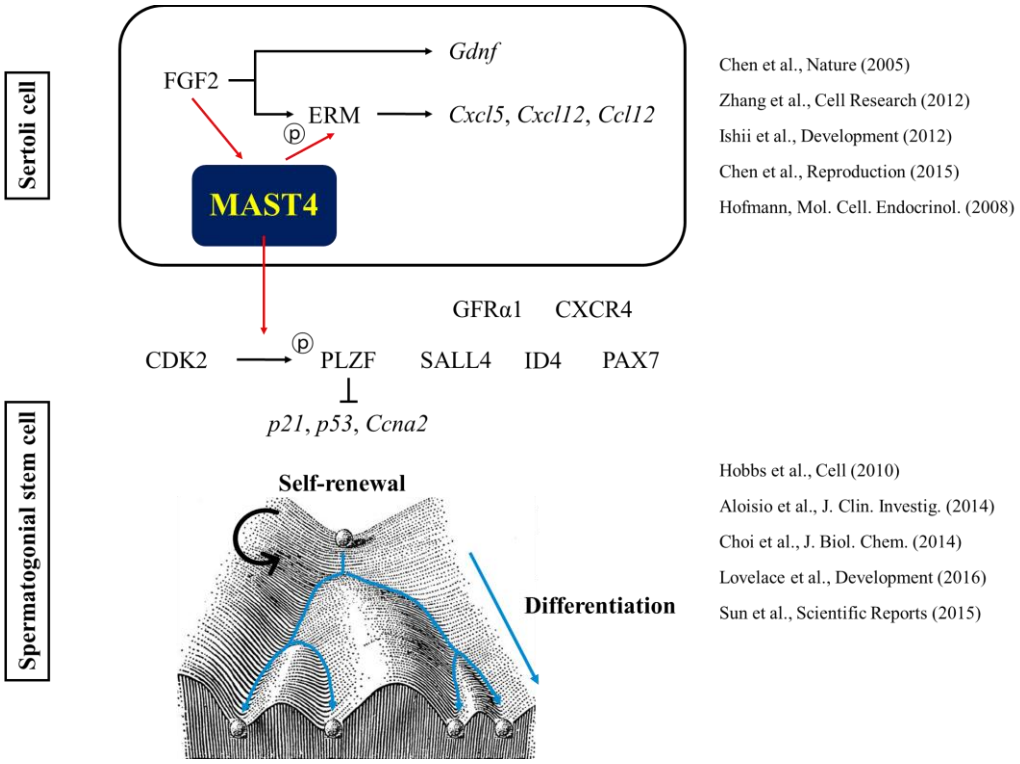

Figure 30. MAST4 regulates the self-renewal of spermatogonial stem cells in terms of cell cycle maintenance through the MAST4-ERM-PLZF mechanism

MAST4 phosphorylates ERM and subsequently regulates the transcription of *Cxcl12*, which is the target gene of ERM in Sertoli cells. CXCL12 migrates to SSCs and transmits the signal involved in SSC self-renewal. CDK2 phosphorylates PLZF that subsequently suppresses the transcription of *Ccna2*. When *Ccna2* transcription is inhibited, SSCs can maintain the cell cycle. *Mast4* KO decreases the transcription of *Cxcl12* and the interaction between PLZF and CDK2. The inhibition of PLZF cannot suppress the transcription of its target genes, and SSCs undergoes cell cycle arrest.

VII. REFERENCES

Ali F, Hindley C, McDowell G, Deibler R, Jones A, et al. 2011. Cell cycle-regulated multi-site phosphorylation of Neurogenin 2 coordinates cell cycling with differentiation during neurogenesis. *Development* 138: 4267-77

Aloisio GM, Nakada Y, Saatcioglu HD, Peña CG, Baker MD, et al. 2014. PAX7 expression defines germline stem cells in the adult testis. *The Journal of clinical investigation* 124: 3929-44

Amiri N, Mohammadi P, Allahgholi A, Salek F, Amini E. 2022. The potential of sertoli cells (SCs) derived exosomes and its therapeutic efficacy in male reproductive disorders. *Life Sciences*: 121251

Barker N, Van Es JH, Kuipers J, Kujala P, Van Den Born M, et al. 2007. Identification of stem cells in small intestine and colon by marker gene Lgr5. *Nature* 449: 1003-07

Bertoli C, Skotheim JM, De Bruin RA. 2013. Control of cell cycle transcription during G1 and S phases. *Nature reviews Molecular cell biology* 14: 518-28

Bianco P. 2014. "Mesenchymal" stem cells. *Annual review of cell and developmental biology* 30: 677-704

Bloch W. 2016. Stem Cell Activation in Adult Organisms. pp. 1005: Multidisciplinary Digital Publishing Institute

Bradley A, Evans M, Kaufman MH, Robertson E. 1984. Formation of germ-line chimaeras from embryo-derived teratocarcinoma cell lines. *Nature* 309: 255-56

Brook F, Gardner R. 1997. The origin and efficient derivation of embryonic stem cells in the mouse. *Proceedings of the National Academy of Sciences* 94: 5709-12

Bryder D, Rossi DJ, Weissman IL. 2006. Hematopoietic stem cells: the paradigmatic tissue-specific stem cell. *The American journal of pathology* 169: 338-46

BÜHRING HJ, Battula VL, Treml S, Schewe B, Kanz L, Vogel W. 2007. Novel markers for the prospective isolation of human MSC. *Ann. N. Y. Acad. Sci.* 1106: 262-71

Chauhan S, Diril MK, Lee JH, Bisteau X, Manoharan V, et al. 2016. Cdk2 catalytic activity is essential for meiotic cell division in vivo. *Biochemical Journal* 473: 2783-98

Chen C, Ouyang W, Grigura V, Zhou Q, Carnes K, et al. 2005. ERM is required for transcriptional control of the spermatogonial stem cell niche. *Nature* 436: 1030-34

Chen S-R, Liu Y-X. 2015. Regulation of spermatogonial stem cell self-renewal and spermatocyte meiosis by Sertoli cell signaling. *Reproduction* 149: R159-R67

Chen T, Wang Y, Tian L, Guo X, Xia J, et al. 2022. Aberrant gene expression profiling in men with Sertoli cell-only syndrome. *Front. Immunol.* 13: 821010

Chen X, Zhang T, Shi J, Xu P, Gu Z, et al. 2013. Notch1 signaling regulates the proliferation and self-renewal of human dental follicle cells by modulating the G1/S phase transition and telomerase activity. *PLoS One* 8: e69967

Choi W-I, Kim M-Y, Jeon B-N, Koh D-I, Yun C-O, et al. 2014. Role of promyelocytic leukemia zinc finger (PLZF) in cell proliferation and cyclin-dependent kinase inhibitor 1A (p21WAF/CDKN1A) gene repression. *Journal of Biological Chemistry* 289: 18625-40

Clevers H. 2005. Stem cells, asymmetric division and cancer. *Nature genetics* 37: 1027-28

Clevers H. 2013. The intestinal crypt, a prototype stem cell compartment. *Cell* 154: 274-84

Cong L, Ran FA, Cox D, Lin S, Barretto R, et al. 2013. Multiplex genome engineering using CRISPR/Cas systems. *Science* 339: 819-23

Costoya J, Hobbs R, Pandolfi P. 2008. Cyclin-dependent kinase antagonizes promyelocytic leukemia zinc-finger through phosphorylation. *Oncogene* 27: 3789-96

Costoya JA, Hobbs RM, Barna M, Cattoretti G, Manova K, et al. 2004. Essential role of Plzf in maintenance of spermatogonial stem cells. *Nature genetics* 36: 653-59

Dabaja AA, Schlegel PN. 2013. Microdissection testicular sperm extraction: an update. *Asian journal of andrology* 15: 35

De Rooij DG. 2017. The nature and dynamics of spermatogonial stem cells. *Development* 144: 3022-30

Du X, Wu S, Wei Y, Yu X, Ma F, et al. 2021. PAX7 promotes CD49f-positive dairy goat spermatogonial stem cells' self-renewal. *Journal of Cellular Physiology* 236: 1481-93

Eistetter HR. 1989. Pluripotent Embryonal Stem Cell Lines Can Be Established from Disaggregated Mouse Morulae: (mouse embryonal stem (ES) cells/disaggregated morulae/in vitro development/teratoma). *Development, growth & differentiation* 31: 275-82

Endo T, Mikedis MM, Nicholls PK, Page DC, de Rooij DG. 2019. Retinoic acid and germ cell development in the ovary and testis. *Biomolecules* 9: 775

Fayomi AP, Orwig KE. 2018. Spermatogonial stem cells and spermatogenesis in mice, monkeys and men. *Stem cell research* 29: 207-14

Garland P, Quraishe S, French P, O'Connor V. 2008. Expression of the MAST family of serine/threonine kinases. *Brain research* 1195: 12-19

Gavet O, Pines J. 2010. Progressive activation of CyclinB1-Cdk1 coordinates entry to mitosis. *Developmental cell* 18: 533-43

Gifford CA, Ranade SS, Samarakoon R, Salunga HT, De Soysa TY, et al. 2019. Oligogenic inheritance of a human heart disease involving a genetic modifier. *Science* 364: 865-70

Gongol B, Marin TL, Jeppson JD, Mayagoitia K, Shin S, et al. 2017. Cellular hormetic response to 27-hydroxycholesterol promotes neuroprotection through AICD induction of MAST4 abundance and kinase activity. *Scientific reports* 7: 1-11

Guo J, Nie X, Giebler M, Mlcochova H, Wang Y, et al. 2020. The Dynamic Transcriptional Cell Atlas of Testis Development during Human Puberty. *Cell Stem Cell*

Harris L, Zalucki O, Piper M. 2018. BrdU/EdU dual labeling to determine the cell-cycle dynamics of defined cellular subpopulations. *J. Mol. Histol.* 49: 229-34

Hasegawa K, Saga Y. 2014. FGF8-FGFR1 signaling acts as a niche factor for maintaining undifferentiated spermatogonia in the mouse. *Biology of reproduction* 91: 145, 1-8

Helsel AR, Yang Q-E, Oatley MJ, Lord T, Sablitzky F, Oatley JM. 2017. ID4 levels dictate the stem cell state in mouse spermatogonia. *Development* 144: 624-34

Hobbs RM, Fagoonee S, Papa A, Webster K, Altruda F, et al. 2012. Functional antagonism between Sall4 and Plzf defines germline progenitors. *Cell stem cell* 10: 284-98

Hu Y-C, Okumura LM, Page DC. 2013. Gata4 is required for formation of the genital ridge in mice. *PLoS genetics* 9: e1003629

Hughes W, Bond V, Brecher G, Cronkite E, Painter R, et al. 1958. Cellular proliferation in the mouse as revealed by autoradiography with tritiated thymidine. *Proceedings of the National Academy of Sciences* 44: 476-83

Ishii K, Kanatsu-Shinohara M, Toyokuni S, Shinohara T. 2012. FGF2 mediates mouse spermatogonial stem cell self-renewal via upregulation of Etv5 and Bcl6b through MAP2K1 activation. *Development* 139: 1734-43

Kar S. 2016. Unraveling cell-cycle dynamics in cancer. *Cell systems* 2: 8-10

Kunisaki Y, Bruns I, Scheiermann C, Ahmed J, Pinho S, et al. 2013. Arteriolar niches maintain haematopoietic stem cell quiescence. *Nature* 502: 637-43

Lane SW, Williams DA, Watt FM. 2014. Modulating the stem cell niche for tissue regeneration. *Nature biotechnology* 32: 795-803

Lau X, Munusamy P, Ng MJ, Sangrithi M. 2020. Single-Cell RNA Sequencing of the Cynomolgus Macaque Testis Reveals Conserved Transcriptional Profiles during Mammalian Spermatogenesis. *Developmental Cell*

Lavery R, Lardenois A, Ranc-Jianmotamedi F, Pauper E, Gregoire EP, et al. 2011. XY Sox9 embryonic loss-of-function mouse mutants show complete sex reversal and produce partially fertile XY oocytes. *Developmental biology* 354: 111-22

Li A, Eirín-López JM, Ausió J. 2005. H2AX: tailoring histone H2A for chromatin-dependent genomic integrity. *Biochem. Cell Biol.* 83: 505-15

Li H, Collado M, Villasante A, Matheu A, Lynch CJ, et al. 2012a. p27Kip1 directly represses Sox2 during embryonic stem cell differentiation. *Cell stem cell* 11: 845-52

Li L, Wang J, Hou J, Wu Z, Zhuang Y, et al. 2012b. Cdk1 interplays with Oct4 to repress differentiation of embryonic stem cells into trophectoderm. *FEBS Lett.* 586: 4100-07

Lim S, Kaldis P. 2013. Cdks, cyclins and CKIs: roles beyond cell cycle regulation. *Development* 140: 3079-93

Liu L, Michowski W, Kolodziejczyk A, Sicinski P. 2019. The cell cycle in stem cell proliferation, pluripotency and differentiation. *Nature cell biology* 21: 1060-67

Lo Celso C, Fleming HE, Wu JW, Zhao CX, Miake-Lye S, et al. 2009. Live-animal tracking of individual haematopoietic stem/progenitor cells in their niche. *Nature* 457: 92-96

Loh Y-H, Wu Q, Chew J-L, Vega VB, Zhang W, et al. 2006. The Oct4 and Nanog transcription network regulates pluripotency in mouse embryonic stem cells. *Nature genetics* 38: 431-40

Lovelace DL, Gao Z, Mutoji K, Song YC, Ruan J, Hermann BP. 2016. The regulatory repertoire of PLZF and SALL4 in undifferentiated spermatogonia. *Development* 143: 1893-906

Loveland KL, Klein B, Pueschl D, Indumathy S, Bergmann M, et al. 2017. Cytokines in male fertility and reproductive pathologies: immunoregulation and beyond. *Front. Endocrinol. (Lausanne)* 8: 307

Malumbres M, Barbacid M. 2001. To cycle or not to cycle: a critical decision in cancer. *Nature reviews cancer* 1: 222-31

Marqués-Torrejón MÁ, Porlan E, Banito A, Gómez-Ibarlucea E, Lopez-Contreras AJ, et al. 2013. Cyclin-dependent kinase inhibitor p21 controls adult neural stem cell expansion by regulating Sox2 gene expression. *Cell stem cell* 12: 88-100

Martynoga B, Morrison H, Price DJ, Mason JO. 2005. Foxg1 is required for specification of ventral telencephalon and region-specific regulation of dorsal telencephalic precursor proliferation and apoptosis. *Developmental biology* 283: 113-27

McConnell MJ, Chevallier N, Berkofsky-Fessler W, Giltnane JM, Malani RB, et al. 2003. Growth Suppression by Acute PromyelocyticLeukemia-Associated Protein PLZF Is Mediated by Repression ofc-mycExpression. *Molecular and Cellular Biology* 23: 9375-88

Medema JP, Vermeulen L. 2011. Microenvironmental regulation of stem cells in intestinal homeostasis and cancer. *Nature* 474: 318-26

Morgan DO. 2007. *The cell cycle: principles of control*. New science press.

Morrison SJ, Kimble J. 2006. Asymmetric and symmetric stem-cell divisions in development and cancer. *nature* 441: 1068-74

Nakagawa T, Sharma M, Nabeshima Y-i, Braun RE, Yoshida S. 2010. Functional hierarchy and reversibility within the murine spermatogenic stem cell compartment. *Science* 328: 62-67

Nichols J, Smith A. 2009. Naive and primed pluripotent states. *Cell stem cell* 4: 487-92

Nichols J, Zevnik B, Anastassiadis K, Niwa H, Klewe-Nebenius D, et al. 1998. Formation of pluripotent stem cells in the mammalian embryo depends on the POU transcription factor Oct4. *Cell* 95: 379-91

Paduch DA, Hilz S, Grimson A, Schlegel PN, Jedlicka AE, Wright WW. 2019a. Aberrant gene expression by Sertoli cells in infertile men with Sertoli cell-only syndrome. *PLoS One* 14: e0216586

Paduch DA, Hilz S, Grimson A, Schlegel PN, Jedlicka AE, Wright WW. 2019b. Aberrant gene expression by Sertoli cells in infertile men with Sertoli cell-only syndrome. *PloS one* 14

Park O-J, Kim H-J, Woo K-M, Baek J-H, Ryoo H-M. 2010. FGF2-activated ERK mitogen-activated protein kinase enhances Runx2 acetylation and stabilization. *Journal of Biological Chemistry* 285: 3568-74

Parker N, Falk H, Singh D, Fidaleo A, Smith B, et al. 2014. Responses to glial cell line-derived neurotrophic factor change in mice as spermatogonial stem cells form progenitor spermatogonia which replicate and give rise to more differentiated progeny. *Biology of reproduction* 91: 92, 1-9

Pawlowski WP, Cande WZ. 2005. Coordinating the events of the meiotic prophase. *Trends Cell Biol.* 15: 674-81

Pearson R, Fleetwood J, Eaton S, Crossley M, Bao S. 2008. Krüppel-like transcription factors: a functional family. *The international journal of biochemistry & cell biology* 40: 1996-2001

Quinn JC, Molinek M, Martynoga BS, Zaki PA, Faedo A, et al. 2007. Pax6 controls cerebral cortical cell number by regulating exit from the cell

cycle and specifies cortical cell identity by a cell autonomous mechanism. *Developmental biology* 302: 50-65

Rahmoun M, Lavery R, Laurent-Chaballier S, Bellora N, Philip GK, et al. 2017. In mammalian foetal testes, SOX9 regulates expression of its target genes by binding to genomic regions with conserved signatures. *Nucleic acids research* 45: 7191-211

Rey RA, Grinspon RP. 2011. Normal male sexual differentiation and aetiology of disorders of sex development. *Best Practice & Research Clinical Endocrinology & Metabolism* 25: 221-38

Sanz-Navarro M, Seidel K, Sun Z, Bertonnier-Brouty L, Amendt BA, et al. 2018. Plasticity within the niche ensures the maintenance of a Sox2+ stem cell population in the mouse incisor. *Development* 145: dev155929

Sato T, Katagiri K, Gohbara A, Inoue K, Ogonuki N, et al. 2011. In vitro production of functional sperm in cultured neonatal mouse testes. *Nature* 471: 504-07

Satyanarayana A, Berthet C, Lopez-Molina J, Coppola V, Tessarollo L, Kaldis P. 2008. Genetic substitution of Cdk1 by Cdk2 leads to embryonic lethality and loss of meiotic function of Cdk2.

Schlesser HN, Simon L, Hofmann M-C, Murphy KM, Murphy T, et al. 2008. Effects of ETV5 (ets variant gene 5) on testis and body growth, time course of spermatogonial stem cell loss, and fertility in mice. *Biology of reproduction* 78: 483-89

Schuijers J, Clevers H. 2012. Adult mammalian stem cells: the role of Wnt, Lgr5 and R-spondins. *The EMBO journal* 31: 2685-96

Sharma M, Braun RE. 2018. Cyclical expression of GDNF is required for spermatogonial stem cell homeostasis. *Development* 145: dev151555

Sharma M, Srivastava A, Fairfield HE, Bergstrom D, Flynn WF, Braun RE. 2019. Identification of EOMES-expressing spermatogonial stem cells and their regulation by PLZF. *Elife* 8: e43352

Sharpe RM, McKinnell C, Kivlin C, Fisher JS. 2003. Proliferation and functional maturation of Sertoli cells, and their relevance to disorders of testis function in adulthood. *REPRODUCTION-CAMBRIDGE-* 125: 769-84

Shi J, Zhang Y, Tan D, Zhang X, Yan M, et al. 2021. PANDORA-seq expands the repertoire of regulatory small RNAs by overcoming RNA modifications. *Nature cell biology* 23: 424-36

Simon L, Ekman GC, Garcia T, Carnes K, Zhang Z, et al. 2010. ETV5 regulates sertoli cell chemokines involved in mouse stem/progenitor spermatogonia maintenance. *Stem cells* 28: 1882-92

Singh P, Patel RK, Palmer N, Grenier JK, Paduch D, et al. 2019. CDK2 kinase activity is a regulator of male germ cell fate. *Development* 146: dev180273

Song H-W, Wilkinson MF. *Semin. Cell Dev. Biol.2014,* 30: 14-26. Elsevier.

Song W, Shi X, Xia Q, Yuan M, Liu J, et al. 2020. PLZF suppresses differentiation of mouse spermatogonial progenitor cells via binding of differentiation associated genes. *Journal of cellular physiology* 235: 3033-42

Sun F, Xu Q, Zhao D, Chen CD. 2015. Id4 marks spermatogonial stem cells in the mouse testis. *Scientific reports* 5: 17594

Sun L, Gu S, Li X, Sun Y, Zheng D, et al. 2006. Identification of a novel human MAST4 gene, a new member of human microtubule associated serine/threonine kinase family. *Molecular Biology* 40: 724-31

Takahashi K, Yamanaka S. 2006. Induction of pluripotent stem cells from mouse embryonic and adult fibroblast cultures by defined factors. *cell* 126: 663-76

Takashima S, Kanatsu-Shinohara M, Tanaka T, Morimoto H, Inoue K, et al. 2015. Functional differences between GDNF-dependent and FGF2-dependent mouse spermatogonial stem cell self-renewal. *Stem cell reports* 4: 489-502

Tavazoie M, Van der Veken L, Silva-Vargas V, Louissaint M, Colonna L, et al. 2008. A specialized vascular niche for adult neural stem cells. *Cell stem cell* 3: 279-88

Tsai YC, Kuo TN, Chao YY, Lee PR, Lin RC, et al. 2023. PDGF-AA activates AKT and ERK signaling for testicular interstitial Leydig cell growth via primary cilia. *J. Cell. Biochem.* 124: 89-102

Van Der Flier LG, Clevers H. 2009. Stem cells, self-renewal, and differentiation in the intestinal epithelium. *Annu. Rev. Physiol.* 71: 241-60

van Velthoven CT, Rando TA. 2019. Stem cell quiescence: dynamism, restraint, and cellular idling. *Cell stem cell* 24: 213-25

Viera A, Alsheimer M, Gómez R, Berenguer I, Ortega S, et al. 2015. CDK2 regulates nuclear envelope protein dynamics and telomere attachment in mouse meiotic prophase. *Journal of cell science* 128: 88-99

Watanabe N, Broome M, Hunter T. 1995. Regulation of the human WEE1Hu CDK tyrosine 15-kinase during the cell cycle. *The EMBO journal* 14: 1878-91

White J, Dalton S. 2005. Cell cycle control of embryonic stem cells. *Stem cell reviews* 1: 131-38

Wobus AM, Boheler KR. 2005. Embryonic stem cells: prospects for developmental biology and cell therapy. *Physiol. Rev.* 85: 635-78

Wu X, Shen Q-T, Oristian DS, Lu CP, Zheng Q, et al. 2011. Skin stem cells orchestrate directional migration by regulating microtubule-ACF7 connections through GSK3β. *Cell* 144: 341-52

Yang R, Liu F, Wang J, Chen X, Xie J, Xiong K. 2019. Epidermal stem cells in wound healing and their clinical applications. *Stem Cell. Res. Ther.* 10: 1-14

Yang Y, Feng Y, Feng X, Liao S, Wang X, et al. 2016. BMP4 cooperates with retinoic acid to induce the expression of differentiation markers in cultured mouse spermatogonia. *Stem cells international* 2016

Yeyati PL, Shaknovich R, Boterashvili S, Li J, Ball HJ, et al. 1999. Leukemia translocation protein PLZF inhibits cell growth and expression of cyclin A. *Oncogene* 18: 925-34

Zhang Y, Wang S, Wang X, Liao S, Wu Y, Han C. 2012. Endogenously produced FGF2 is essential for the survival and proliferation of cultured mouse spermatogonial stem cells. *Cell research* 22: 773-76

Zhou Q, Chipperfield H, Melton DA, Wong WH. 2007. A gene regulatory network in mouse embryonic stem cells. *Proceedings of the National Academy of Sciences* 104: 16438-43

Zwaka TP, Thomson JA. 2005. A germ cell origin of embryonic stem cells?

ABSTRACT (In Korean)

FGF2/ERM 신호전달경로 및 세포주기 조절을 통한 MAST4 의 정원줄기세포 자가재생 기전 구명

이승준

연세대학교 대학원

응용생명과학과

정자형성과정은 남성의 수명 전반에 걸쳐 배우자를 생성하고 활성 상태를 유지하는 중요한 세포 분화 과정이다. 세르톨리세포단독증후군은 불임을 포함한 남성 생식 기관의 기능 장애를 말하고, 이를 예방하려면 정원줄기세포의 정확한 자가재생이 필수적이다. 본 연구는 생쥐의 정자형성과정에서 MAST4 의 역할에 대해 제시하였다. MAST4 는 사춘기 이전 세르톨리세포에 발현되어 생쥐의 정자형성과정을 위한 미세환경을 제공했다. *Mast4* 녹아웃 정소는 야생형 정소에 비해 크기가 감소했으며, 세포사멸의 증가 및 그에 따른 정세관 구조의 손실과 관련된 생식세포의 고갈은 세르톨리세포단독증후군의 표현형과 유사했다. 기존에 세르톨리세포에 발현되는 ERM 단백질은 FGF2 신호전달경로에 의해 조절되어 정원줄기세포의 자가재생을 유도하였다.

본 연구에서 MAST4 또한 FGF2 의 조절을 받으며 ERM 의 세린 367 잔기를 인산화했다. ERM 의 인산화는 궁극적으로 정원줄기세포의 자가재생과 관련된 ERM 타겟 유전자의 전사를 조절했다. *Mast4* 유전자의 결실은 정소에서 PLZF 의 발현 및 정원줄기세포의 세포주기 진행을 감소시켰다. MAST4 는 또한 CDK2 를 유도하여 PLZF 를 인산화시켰고, 활성화된 PLZF 는 세포주기 정지와 관련된 유전자의 전사를 억제하여 정원줄기세포가 줄기세포 상태를 유지할 수 있도록 유도했다. 따라서 MAST4 는 FGF2/ERM 신호전달경로와 연관되어 있으며 이 연관은 척추동물의 줄기세포 미세환경을 유지하는 정원줄기세포의 능력을 탐구하는 데 도움이 된다. 또한 MAST4 를 통한 불임 예방과 다른 상피성 기관의 줄기세포 자가재생에도 중요한 역할을 할 것을 시사한다.

핵심되는 말: MAST4, 정원줄기세포 자가재생, 줄기세포 미세환경, 세포주기, 세르톨리세포단독증후군

PUBLICATION LIST

Lee SJ, Park J, Lee DJ, Otsu K, Kim P, Mizuno S, Lee MJ, Kim HY, Harada H, Takahashi S, Kim SJ, Jung HS. 2021. *Mast4* knockout shows the regulation of spermatogonial stem cell self-renewal via the FGF2/ERM pathway. Cell Death and Differentiation. 28(5):1441-1454.

Lee SJ, Kim KH, Lee DJ, Kim P, Park J, Kim SJ, Jung HS. 2023. MAST4 controls cell cycle in spermatogonial stem cels. Cell Proliferation. 56(4):e13390.